Quadratic and Cubic Nonlinear Optical Properties of Salts of Diquat-Based Chromophores with Diphenylamino Substituents

Benjamin J. Coe,*,† John Fielden,† Simon P. Foxon,† Madeleine Helliwell,† Bruce S. Brunschwig,‡ Inge Asselberghs,§ Koen Clays,§ Joanna Olesiak,|| Katarzyna Matczyszyn,|| and Marek Samoc||,#

School of Chemistry, University of Manchester, Oxford Road, Manchester M13 9PL, U.K., Molecular Materials Research Center, Beckman Institute, MC 139-74, California Institute of Technology, 1200 East California Boulevard, Pasadena, California 91125, United States, Department of Chemistry, University of Leuven, Celestijnenlaan 200D, B-3001 Leuven, Belgium, Institute of Physical and Theoretical Chemistry, Wrocław University of Technology, Wybrzeże Wyspiańskiego 27, 50-370 Wrocław, Poland and Laser Physics Centre, Research School of Physics and Engineering, Australian National University, Canberra ACT 0200, Australia

Received: July 13, 2010

A series of chromophoric salts has been prepared in which 4-(diphenylamino)phenyl (Dpap) electron donor groups are connected to electron-accepting diquaternized 2,2′-bipyridyl (diquat) units. The main aim is to combine large quadratic and cubic nonlinear optical (NLO) effects in potentially redox-switchable molecules with 2D structures. The chromophores have been characterized as their PF_6^- salts by using various techniques including electronic absorption spectroscopy and cyclic voltammetry. The visible absorption spectra are dominated by intense $\pi \rightarrow \pi^*$ intramolecular charge-transfer (ICT) bands, and all of the compounds show two reversible or quasireversible diquat-based reductions and partially reversible Dpap oxidations. Single crystal X-ray structures have been obtained for one salt and for the precursor compound (*E*)-4-(diphenylamino)cinnamaldehyde, both of which adopt centrosymmetric space groups. First hyperpolarizabilities β have been measured by using hyper-Rayleigh scattering (HRS) with a 800 nm laser, and Stark (electroabsorption) spectroscopy of the ICT bands affords estimated static first hyperpolarizabilities β_0. The directly and indirectly derived β values are large and generally increased substantially for the bis-Dpap derivatives when compared with their monosubstituted analogues. Polarized HRS studies show that the NLO responses of the disubstituted species are dominated by "off-diagonal" β_{zyy} components. Lengthening the diquaternizing alkyl unit lowers the electron-acceptor strength and therefore increases the ICT energies and decreases the $E_{1/2}$ values for diquat reduction. However, compensating increases in the ICT intensity prevent significant decreases in the Stark-based β_0 responses. Cubic NLO properties have been measured by using the Z-scan technique over a wavelength range of 520−1600 nm, revealing relatively high two-photon absorption cross-sections of up to 730 GM at 620 nm for one of the disubstituted chromophores.

1. Introduction

Organic compounds containing pyridinium units are of longstanding interest from a diverse range of perspectives, including applications in electronic/optical devices.[1] Such compounds are generally synthetically readily accessible, highly stable, and often combine intense absorptions in the visible region (thus dye-like behavior) with reversible electrochemical properties. Just some of the recent interesting studies with such compounds have included observations of aggregation-induced emission,[2] excited-state inclusion into zeolite channels,[3] multielectron redox,[4] ferroelectricity in organic−inorganic hybrid materials,[5] and fluorescent DNA probes for live-cell imaging.[6] However, one of the areas that has proven most fruitful for exploitation of pyridinium salts is that of nonlinear optical (NLO) effects, which is of relevance to various applications such as advanced telecommunications and biological imaging.[7] From this perspective, special attention has been given to compounds such as (*E*)-4′-(dimethylamino)-*N*-methyl-4-stilbazolium tosylate (DAST)[8] and related species.[9] Notably, crystals of DAST have recently been commercialized for THz wave generation via nonlinear frequency mixing,[10] promising applications including security scanning, biomedical analysis, and space communications.[11]

Molecular NLO phenomena are divided into two major classes. So-called quadratic (second-order) behavior arises from the first hyperpolarizability β that translates into the susceptibility $\chi^{(2)}$ in bulk materials. In order to achieve nonzero values of both β and $\chi^{(2)}$, the structure must be noncentrosymmetric at the molecular and macroscopic levels. Second harmonic generation (SHG) and linear electro-optic behavior are the most widely studied quadratic NLO effects. The other main class of property, cubic (third-order) NLO behavior, is governed by the second hyperpolarizability γ. The bulk counterpart of γ is $\chi^{(3)}$, and while this parameter has nonzero values for any symmetry, its magnitude is affected by the macroscopic structure of a material. Potentially useful for applications including optical power limiting, 3D optical data storage, and photodynamic cancer therapy, two-photon absorption (2PA) derives from the γ

* To whom correspondence should be addressed. Fax: 44 161-275-4598. E-mail: b.coe@manchester.ac.uk.
† University of Manchester.
‡ California Institute of Technology.
§ University of Leuven.
|| Wrocław University of Technology.
Australian National University.

10.1021/jp106473e
Published on Web 10/26/2010

response.[12] Molecules with large β values typically feature π-electron donor (π-ED) and acceptor (π-EA) groups linked via a polarizable π-system, the π-EA function being the pyridinium rings in compounds like DAST. In principle, cubic NLO effects can arise from any material, but the primary requirement for a large γ value is simply an extended π-system.

Hyperpolarizabilities are third- (β) or fourth-rank (γ) tensors that can have a number of nonzero components. Although most NLO molecules are simple 1D dipoles, multidimensional species including 2D dipoles and octupoles are also highly interesting.[13,14] Such chromophores can offer significant potential advantages over their 1D counterparts, including enhanced NLO responses without undesirable losses of visible transparency. In V-shaped species, having more than one significant component of β can prevent reabsorption of SHG that can be polarized perpendicular to the $\pi \rightarrow \pi^*$ intramolecular charge-transfer (ICT) transition dipole moment (μ_{12}); phase-matching between the fundamental and harmonic waves may also be facilitated.[13a]

We have previously studied salts of chromophores containing diquaternized 2,2′-bipyridyl (diquat, DQ^{2+}) units.[15] Except for one brief theoretical report relating to 2PA,[16] DQ^{2+} groups had not been used for NLO purposes previously. Such tricyclic moieties are stronger π-EAs than simple pyridinium groups, allow the creation of 2D dipoles and show reversible reductions that may allow redox-switching of the optical properties. Our previous reports concerned only the quadratic NLO properties of chromophores with 4-(dimethylamino)phenyl (Dmap) or julolidinyl (Jd) π-ED groups, showing very large and strongly 2D β responses.[15] Here we describe a series of closely related compounds that contain instead 4-(diphenylamino)phenyl (Dpap) groups, including measurements of both quadratic and cubic NLO effects. We chose to focus on these triarylamine derivatives for 2PA studies because they contain larger π-systems when compared with their Dmap or Jd analogues.

2. Experimental Section

2.1. Materials and Procedures. Dichloromethane and acetonitrile were dried over CaH_2 and distilled under argon. All other reagents and solvents were obtained as ACS grade from Sigma Aldrich, Alfa Aesar, or Fisher Scientific and were used as supplied. The compounds 4-[(diethoxyphosphinyl)methyl]-4′-methyl-2,2′-bipyridyl,[17] 4,4′-bis-[(diethoxyphosphinyl)methyl]-2,2′-bipyridyl,[18] 1,2-bis(triflyloxy)ethane,[19] and 1,3-bis(triflyloxy)propane[19] were synthesized by following previously published methods. Products were dried at room temperature overnight in a vacuum desiccator ($CaSO_4$) prior to characterization.

2.2. General Physical Measurements. ^{1}H NMR spectra were recorded on Bruker UltraShield 500, AV-400, or DPX-300 spectrometers, and all shifts are quoted with respect to TMS. The fine splitting of pyridyl or phenyl ring AA′BB′ patterns is ignored, and the signals are reported as simple doublets, with J values referring to the two most intense peaks. Abbreviations used: ax = axial; eq = equatorial. Elemental analyses were performed by the Microanalytical Laboratory, University of Manchester using a Carlo Erba EA1108 instrument. UV−vis spectra were obtained by using a Shimadzu UV-2401 PC spectrophotometer, and mass spectra were recorded by using +electrospray on a Micromass Platform II spectrometer. The IR spectrum of Dpaca was obtained by using the pure solid on a Varian Bio-Rad Excalibur series spectrometer. Cyclic voltammetric measurements were performed by using an EG&G PAR model 283, Autolab PGStat 100 or Ivium CompactStat potentiostat/galvanostat. A single-compartment cell was used with a silver/silver chloride reference electrode (3 M NaCl, saturated AgCl) separated by a salt bridge from a 2 mm glassy carbon disk working electrode and Pt wire auxiliary electrode. Acetonitrile was freshly distilled (from CaH_2), and $[N(C_4H_9\text{-}n)_4]PF_6$, as supplied from Fluka, was used as the supporting electrolyte. Solutions containing ca. 10^{-3} M analyte (0.1 M electrolyte) were deaerated by purging with N_2. All $E_{1/2}$ values were calculated from $(E_{pa} + E_{pc})/2$ at a scan rate of 200 mV s^{-1}.

2.3. Synthesis of (*E*)-4-(Diphenylamino)cinnamaldehyde, Dpaca. 4-(Diphenylamino)benzaldehyde (500 mg, 1.83 mmol) and 1,3-dioxan-2-yl-tributylphosphonium bromide (3.0 mL, 1.2 M, 3.60 mmol) were dissolved in anhydrous THF (30 mL). Sodium hydride (125 mg, 5.21 mmol) was added with a catalytic amount of 18-crown-6, and the suspension was stirred for 22 h at room temperature. Water (25 mL) was added to the mixture, and the mixture was extracted with diethyl ether (3 × 25 mL). The extracts were combined and concentrated under vacuum to afford a yellow oil. This material was dissolved in THF (25 mL), 10% hydrochloric acid (25 mL) was added, and the solution was stirred for 1 h at room temperature. The solution was extracted with dichloromethane (3 × 25 mL), and the extracts were combined and concentrated under vacuum to give a yellow solid that was purified via column chromatography on silica gel with dichloromethane as eluant. The major yellow band was collected, evaporated to dryness under vacuum and dried to give a golden powder: 507 mg, 91%; δ_H (500 MHz, $CDCl_3$) 9.64 (1 H, d, J = 8.0 Hz, CHO), 7.41−7.37 (3 H, CH + C_6H_4), 7.33−7.30 (4 H, Ph), 7.15−7.11 (6 H, Ph), 7.01 (2 H, d, J = 8.5 Hz, C_6H_4), 6.59 (1 H, dd, J = 15.8, 7.8 Hz, CH). Anal. Calcd. (%) for $C_{21}H_{17}NO \cdot 0.2H_2O$: C, 83.25; H, 5.79; N, 4.62. Found: C, 83.54; H, 5.92; N, 4.52. m/z = 300.0 (MH^+). Note: the duration of the column chromatography affects the isolated yield, which is optimized by using a relatively short silica path length (ca. 8−10 cm) and a rapid elution rate. The loss of product observed when allowing the material to remain on the silca gel for prolonged periods may be attributable to facile aerial oxidation to the corresponding carboxylic acid that is expected to have an especially high affinity for oxide surfaces.

2.4. Synthesis of 4-[(*E*)-2-(4-Diphenylaminophenyl)ethenyl]-4′-methyl-2,2′-bipyridyl (1). Potassium *tert*-butoxide (117 mg, 1.043 mmol) was added to a solution of 4-[(diethoxyphosphinyl)methyl]-4′-methyl-2,2′-bipyridyl (240 mg, 0.749 mmol) and 4-(diphenylamino)benzaldehyde (205 mg, 0.750 mmol) stirred in THF (20 mL), resulting in near instantaneous production of a yellow precipitate. After stirring at room temperature for 5 h, water (20 mL) was added to the mixture, and the THF was removed under vacuum. The yellow product was filtered off, washed with cold water, and dried: 293 mg, 88%; δ_H (500 MHz, $CDCl_3$) 8.62 (1 H, d, J = 5.4 Hz, C_5H_3N), 8.58 (1 H, d, J = 4.7 Hz, C_5H_3N), 8.49 (1 H, s, C_5H_3N), 8.27 (1 H, s, C_5H_3N), 7.44−7.38 (3 H, C_6H_4 + CH), 7.35 (1 H, d, J = 5.0 Hz, C_5H_3N), 7.29 (4 H, t, J = 7.4 Hz, Ph), 7.17−7.13 (5 H, C_5H_3N + Ph), 7.09−7.05 (4 H, C_6H_4 + Ph), 7.01 (1 H, d, J = 16.4 Hz, CH), 2.38 (3 H, s, Me). ν(C═O) 1664s cm^{-1}. Anal. Calcd (%) for $C_{31}H_{25}N_3 \cdot 0.25H_2O$: C, 83.85; H, 5.79; N, 9.46. Found: C, 84.21; H, 5.73; N, 9.11. m/z = 440.2 (MH^+).

2.5. Synthesis of 4-[(*E,E*)-4-(4-Diphenylaminophenyl)buta-1,3-dienyl]-4′-methyl-2,2′-bipyridyl (2). This compound was prepared in a manner similar to **1** by using potassium *tert*-butoxide (93 mg, 0.829 mmol), 4-[(diethoxyphosphinyl)methyl]-4′-methyl-2,2′-bipyridyl (190 mg, 0.593 mmol), and Dpaca (178 mg, 0.593 mmol) in place of 4-(diphenylamino)benzaldehyde. The product was obtained as a golden solid: 222 mg, 78%; δ_H (500 MHz, CD_3CN + CF_3CO_2D) 8.64 (1 H, d, J = 5.4 Hz,

C_5H_3N), 8.56 (1 H, d, $J = 6.0$ Hz, C_5H_3N), 8.44 (1 H, s, C_5H_3N), 8.33 (1 H, s, C_5H_3N), 7.79 (1 H, d, $J = 6.3$ Hz, C_5H_3N), 7.73−7.66 (1 H, m, CH), 7.61 (1 H, d, $J = 6.0$ Hz, C_5H_3N), 7.47 (2 H, d, $J = 7.9$ Hz, C_6H_4), 7.34 (4 H, t, $J = 7.9$ Hz, Ph), 7.15−7.09 (6 H, Ph), 7.08−7.00 (2 H, 2CH), 6.96 (2 H, d, $J = 7.9$ Hz, C_6H_4), 6.80 (1 H, d, $J = 15.1$ Hz, CH), 2.59 (3 H, s, Me). Anal. Calcd (%) for $C_{33}H_{27}N_3 \cdot 0.7H_2O$: C, 82.88; H, 5.99; N, 8.79. Found: C, 82.93; H, 5.88; N, 8.44. $m/z = 466.2$ (MH^+).

2.6. Synthesis of 4,4′-Bis-[(*E*)-2-(4-diphenylaminophenyl)ethenyl]-2,2′-bipyridyl (3). This compound was prepared in a manner similar to **1** by using potassium *tert*-butoxide (312 mg, 2.78 mmol), 4,4′-bis-[(diethoxyphosphinyl)methyl]-2,2′-bipyridyl (500 mg, 1.10 mmol) in place of 4-[(diethoxyphosphinyl)methyl]-4′-methyl-2,2′-bipyridyl, and 4-(diphenylamino)benzaldehyde (599 mg, 2.19 mmol) to afford a golden solid: 760 mg, 97%; δ_H (500 MHz, $CDCl_3$) 8.65 (2 H, d, $J = 5.4$ Hz, C_5H_3N), 8.52 (2 H, s, C_5H_3N), 7.44 (4 H, d, $J = 8.5$ Hz, $2C_6H_4$), 7.42 (2 H, d, $J = 16.1$ Hz, 2CH), 7.38 (2 H, d, $J = 5.0$ Hz, C_5H_3N), 7.29 (8 H, t, $J = 7.9$ Hz, Ph), 7.14 (8 H, d, $J = 7.6$ Hz, Ph), 7.10−7.06 (8 H, $2C_6H_4$ + Ph), 7.02 (2 H, d, $J = 16.1$ Hz, 2CH). Anal. Calcd (%) for $C_{50}H_{38}N_4 \cdot H_2O$: C, 84.24; H, 5.66; N, 7.86. Found: C, 84.37; H, 5.75; N, 7.55.

2.7. Synthesis of 4,4′-Bis-[(*E,E*)-4-(4-diphenylaminophenyl)buta-1,3-dienyl]-2,2′-bipyridyl (4). This compound was prepared in a manner similar to **3** by using Dpaca (656 mg, 2.19 mmol) in place of 4-(diphenylamino)benzaldehyde. The mixture was washed with a small amount of methanol, and a golden solid was obtained: 737 mg, 88%; δ_H (500 MHz, $CDCl_3$) 8.63 (2 H, d, $J = 5.4$ Hz, C_5H_3N), 8.44 (2 H, s, C_5H_3N), 7.35 (4 H, d, $J = 8.5$ Hz, $2C_6H_4$), 7.32−7.27 (12 H, Ph + 2CH + C_3H_5N), 7.13 (8 H, d, $J = 8.2$ Hz, Ph), 7.08−7.02 (8 H, $2C_6H_4$ + Ph), 6.92−6.85 (2 H, m, 2CH), 6.76 (2 H, d, $J = 16.1$ Hz, 2CH), 6.64 (2 H, $J = 15.5$ Hz, 2CH). Anal. Calcd (%) for $C_{54}H_{42}N_4 \cdot H_2O$: C, 84.79; H, 5.80; N, 7.32. Found: C, 84.83; H, 5.70; N, 7.36.

2.8. Synthesis of 2-Methyl-11-[(*E*)-2-(4-diphenylaminophenyl)ethenyl]-6,7-dihydro-dipyrido[1,2-*a*:2′,1′-*c*]pyrazinediium Hexafluorophosphate (5). To a solution of **1**·0.25H_2O (164 mg, 0.369 mmol) in chloroform (20 mL) was added 1,2-bis(triflyloxy)ethane (242 mg, 0.742 mmol) in dry dichloromethane (2 mL). The reaction was stirred at room temperature for 48 h, during which time the solution color changed to deep purple and a dark precipitate formed. The volume was reduced to ca. 5 mL under vacuum, and diethyl ether was added to the mixture to ensure complete precipitation of the crude triflate salt, which was then filtered off and washed with diethyl ether. This solid was dissolved in methanol, and aqueous NH_4PF_6 was added to precipitate the product, which was then filtered off and washed with water. The dark purple product was purified by reprecipitation from acetonitrile/diethyl ether, filtered off, washed with diethyl ether, and dried: 175 mg, 62%; δ_H (500 MHz, CD_3CN) 8.71 (1 H, d, $J = 6.3$ Hz, C_5H_3N), 8.69 (1 H, s, C_5H_3N), 8.67 (1 H, s, C_5H_3N), 8.56 (1 H, d, $J = 6.3$ Hz, C_5H_3N), 8.07 (1 H, d, $J = 6.6$ Hz, C_5H_3N), 8.05−8.01 (2 H, C_5H_3N + CH), 7.63 (2 H, d, $J = 8.8$ Hz, C_6H_4), 7.40 (4 H, t, $J = 7.5$ Hz, Ph), 7.28−7.18 (7 H, CH + Ph), 7.00 (2 H, d, $J = 8.8$ Hz, C_6H_4), 5.00−4.97 (2 H, m, CH_2), 4.91−4.88 (2 H, m, CH_2), 2.83 (3 H, s, Me). Anal. Calcd (%) for $C_{33}H_{29}F_{12}N_3P_2 \cdot 0.5H_2O$: C, 51.70; H, 3.94; N, 5.48. Found: C, 51.70; H, 3.63; N, 5.45. m/z = 612.4 ($[M - PF_6]^+$), 234.1 ($[M - 2PF_6]^{2+}$).

2.9. Synthesis of 2-Methyl-11-[(*E,E*)-4-(4-diphenylaminophenyl)buta-1,3-dienyl]-6,7-dihydro-dipyrido[1,2-*a*:2′,1′-*c*]pyrazinediium Hexafluorophosphate (6). This compound was prepared in manner similar to **5** by using **2**·0.7H_2O (100 mg, 0.209 mmol) in place of **1**·0.25H_2O with 1,2-bis(triflyloxy)ethane (140 mg, 0.430 mmol). Purification of the crude product (103 mg) was effected by column chromatography on silica gel, eluting with 48:6:1 acetone/water/saturated aqueous KNO_3. The major purple band was collected, and the addition of aqueous NH_4PF_6 afforded a precipitate that was filtered off, washed with water, and dried. Further purification was achieved by reprecipitation from acetonitrile/diethyl ether to afford a dark purple solid: 35 mg, 21%; δ_H (500 MHz, CD_3CN) 8.72 (1 H, d, $J = 6.3$ Hz, C_5H_3N), 8.69 (1 H, s, C_5H_3N), 8.60 (1 H, s, C_5H_3N), 8.55 (1 H, d, $J = 6.6$ Hz, C_5H_3N), 8.07 (1 H, d, $J = 6.3$ Hz, C_5H_3N), 8.00 (1 H, d, $J = 6.6$ Hz, C_5H_3N), 7.94−7.88 (1 H, m, CH), 7.51 (2 H, d, $J = 8.8$ Hz, C_6H_4), 7.36 (4 H, t, $J = 8.0$ Hz, Ph), 7.18−7.11 (8 H, 2CH + Ph), 6.96 (2 H, d, $J = 8.8$ Hz, C_6H_4), 6.85 (1 H, d, $J = 15.5$ Hz, CH), 4.99−4.96 (2 H, m, CH_2), 4.90−4.87 (2 H, m, CH_2), 2.80 (3 H, s, Me). Anal. Calcd (%) for $C_{35}H_{31}F_{12}N_3P_2$: C, 53.65; H, 3.99; N, 5.36. Found: C, 53.49; H, 3.58; N, 5.20. $m/z = 638.3$ ($[M - PF_6]^+$), 246.9 ($[M - 2PF_6]^{2+}$).

2.10. Synthesis of 2-Methyl-12-[(*E*)-2-(4-diphenylaminophenyl)ethenyl]-7,8-dihydro-6*H*-dipyrido[1,2-*a*:2′,1′-*c*]-[1,4]diazepinium Hexafluorophosphate (7). This compound was prepared and purified in manner similar to **5** by using **1**·0.25H_2O (100 mg, 0.225 mmol) with 1,3-bis(triflyloxy)propane (155 mg, 0.456 mmol) in place of 1,2-bis(triflyloxy)ethane to afford a dark purple solid: 90 mg, 52%; δ_H (300 MHz, CD_3CN) 8.76 (1 H, d, $J = 6.4$ Hz, C_5H_3N), 8.59 (1 H, d, $J = 6.6$ Hz, C_5H_3N), 8.23 (1 H, s, C_5H_3N), 8.21 (1 H, s, C_5H_3N), 8.13−8.05 (2 H, C_5H_3N), 7.94 (1 H, d, $J = 16.0$ Hz, CH), 7.61 (2 H, d, $J = 8.7$ Hz, C_6H_4), 7.40 (4 H, t, $J = 7.2$ Hz, Ph), 7.26 (1 H, d, $J = 15.4$ Hz, CH), 7.22−7.17 (6 H, Ph), 6.98 (2 H, d, $J = 8.7$ Hz, C_6H_4), 4.83−4.73 (1 H, m, NCH_2^{eq}), 4.72−4.62 (1 H, m, NCH_2^{eq}), 4.42−4.29 (1 H, m, NCH_2^{ax}), 4.23−4.11 (1 H, m, NCH_2^{ax}), 2.79−2.68 (5 H, Me + CH_2). Anal. Calcd (%) for $C_{34}H_{31}F_{12}N_3P_2$: C, 52.93; H, 4.05; N, 5.45. Found: C, 52.68; H, 3.69; N, 5.22. $m/z = 626.3$ ($[M - PF_6]^+$), 240.9 ($[M - 2PF_6]^{2+}$).

2.11. Synthesis of 2-Methyl-12-[(*E,E*)-4-(4-diphenylaminophenyl)buta-1,3-dienyl]-7,8-dihydro-6*H*-dipyrido[1,2-*a*:2′,1′-*c*]-[1,4]diazepinium Hexafluorophosphate (8). This compound was prepared and purified in manner similar to **7** by using **2**·0.7H_2O (100 mg, 0.209 mmol) in place of **1**·0.25H_2O with 1,3-bis(triflyloxy)propane (146 mg, 0.429 mmol) to afford a dark purple solid: 92 mg, 55%; δ_H (400 MHz, CD_3CN) 8.75 (1 H, d, $J = 6.3$ Hz, C_5H_3N), 8.57 (1 H, d, $J = 6.6$ Hz, C_5H_3N), 8.20 (1 H, s, C_5H_3N), 8.15 (1 H, s, C_5H_3N), 8.11 (1 H, d, $J = 6.3$ Hz, C_5H_3N), 8.02 (1 H, d, $J = 6.6$ Hz, C_5H_3N), 7.85−7.77 (1 H, m, CH), 7.49 (2 H, d, $J = 8.8$ Hz, C_6H_4), 7.36 (4 H, t, $J = 7.4$ Hz, Ph), 7.18−7.10 (8 H, 2CH + Ph), 6.96 (2 H, d, $J = 8.8$ Hz, C_6H_4), 6.84 (1 H, d, $J = 15.4$ Hz, CH), 4.82−4.73 (1 H, m, NCH_2^{eq}), 4.70−4.62 (1 H, m, NCH_2^{eq}), 4.39−4.28 (1 H, m, NCH_2^{ax}), 4.22−4.11 (1 H, m, NCH_2^{ax}), 2.79−2.68 (5 H, Me + CH_2). Anal. Calcd (%) for $C_{36}H_{33}F_{12}N_3P_2$: C, 54.21; H, 4.17; N, 5.27. Found: C, 54.58; H, 4.28; N, 5.23. $m/z = 652.3$ ($[M - PF_6]^+$), 253.9 ($[M - 2PF_6]^{2+}$).

2.12. Synthesis of 2,11-Bis[(*E*)-2-(4-diphenylaminophenyl)ethenyl]-6,7-dihydro-dipyrido[1,2-*a*:2′,1′-*c*]pyrazinediium Hexafluorophosphate (9). This compound was prepared and purified in manner similar to **5** by using **3**·H_2O (100 mg, 0.140 mmol) in place of **1**·0.25H_2O with 1,3-bis(triflyloxy)ethane (94 mg, 0.288 mmol). A dark purple solid was obtained: 76 mg, 53%; δ_H (500 MHz, CD_3CN) 8.84 (2 H, s, C_5H_3N), 8.53 (2 H, d, $J = 6.0$ Hz, C_5H_3N), 8.11 (2 H, d, $J = 15.7$ Hz, 2CH), 8.00 (2 H, d, $J = 6.0$ Hz, C_5H_3N), 7.63 (4 H, d, $J = 8.8$ Hz, $2C_6H_4$), 7.40 (8 H, t, $J = 7.8$ Hz, Ph), 7.29−7.17 (14 H, 2CH + Ph),

6.99 (4 H, d, $J = 8.8$ Hz, $2C_6H_4$), 4.87 (4 H, s, $2CH_2$). Anal. Calcd (%) for $C_{52}H_{42}F_{12}N_4P_2 \cdot H_2O$: C, 60.59; H, 4.30; N, 5.43. Found: C, 60.44; H, 4.13; N, 5.45. $m/z = 867.5$ ($[M - PF_6]^+$), 361.6 ($[M - 2PF_6]^{2+}$).

2.13. Synthesis of 2,11-Bis[(*E,E*)-4-(4-diphenylaminophenyl)buta-1,3-dienyl]-6,7-dihydro-dipyrido[1,2-*a*:2′,1′-*c*]pyrazinediium Hexafluorophosphate (10). This compound was prepared in manner similar to **5** by using $\mathbf{4} \cdot H_2O$ (108 mg, 0.141 mmol) in place of $\mathbf{1} \cdot 0.25H_2O$ with 1,2-bis(triflyloxy)ethane (94 mg, 0.288 mmol). Purification of the crude product (82 mg) was effected as for **6** to afford a dark purple solid: 42 mg, 27%; δ_H (500 MHz, CD_3CN) 8.65 (2 H, s, C_5H_3N), 8.52 (2 H, d, $J = 6.3$ Hz, C_5H_3N), 7.99 (2 H, d, $J = 6.6$ Hz, C_5H_3N), 7.96−7.90 (2 H, m, 2CH), 7.52 (4 H, d, $J = 8.5$ Hz, $2C_6H_4$), 7.36 (8 H, t, $J = 7.7$ Hz, Ph), 7.19−7.11 (16 H, 4CH + Ph), 6.97 (4 H, d, $J = 8.5$ Hz, $2C_6H_4$), 6.86 (2 H, d, $J = 15.5$ Hz, 2CH), 4.85 (4 H, s, $2CH_2$). Anal. Calcd (%) for $C_{56}H_{46}F_{12}N_3P_2 \cdot 1.9H_2O$: C, 61.19; H, 4.57; N, 5.10. Found: C, 61.21; H, 4.31; N, 5.07. $m/z = 919.6$ ($[M - PF_6]^+$), 387.6 ($[M - 2PF_6]^{2+}$).

2.14. Synthesis of 2,12-Bis[(*E*)-2-(4-diphenylaminophenyl)ethenyl]-7,8-dihydro-6*H*-dipyrido[1,2-*a*:2′,1′-*c*]-[1,4]diazepinium Hexafluorophosphate (11). This compound was prepared and purified in a manner similar to **5** by using $\mathbf{3} \cdot H_2O$ (100 mg, 0.140 mmol) in place of $\mathbf{1} \cdot 0.25H_2O$ and 1,3-bis(triflyloxy)propane (94 mg, 0.276 mmol) in place of 1,2-bis(triflyloxy)ethane. A dark purple solid was obtained: 63 mg, 43%; δ_H (500 MHz, CD_3CN) 8.58 (2 H, d, $J = 6.6$ Hz, C_5H_3N), 8.31 (2 H, s, C_5H_3N), 8.06 (2 H, d, $J = 6.0$ Hz, C_5H_3N), 7.95 (2 H, d, $J = 16.4$ Hz, 2CH), 7.61 (4 H, d, $J = 8.5$ Hz, $2C_6H_4$), 7.39 (8 H, t, $J = 7.7$ Hz, Ph), 7.27 (2 H, d, $J = 15.8$ Hz, 2CH), 7.23−7.15 (12 H, Ph), 6.98 (4 H, d, $J = 8.5$ Hz, $2C_6H_4$), 4.71−4.64 (2 H, m, NCH_2^{eq}), 4.31−4.22 (2 H, m, NCH_2^{ax}), 2.74−2.67 (2 H, m, CH_2). Anal. Calcd (%) for $C_{53}H_{44}F_{12}N_4P_2 \cdot 0.7H_2O$: C, 61.24; H, 4.40; N, 5.39. Found: C, 61.22; H, 4.20; N, 5.52. $m/z = 881.9$ ($[M - PF_6]^+$), 368.5 ($[M - 2PF_6]^{2+}$).

2.15. Synthesis of 2,12-Bis[(*E,E*)-4-(4-diphenylaminophenyl)buta-1,3-dienyl]-7,8-dihydro-6*H*-dipyrido[1,2-*a*:2′,1′-*c*]-[1,4]diazepinium Hexafluorophosphate (12). This compound was prepared and purified in manner similar to **11** by using $\mathbf{4} \cdot H_2O$ (108 mg, 0.141 mmol) in place of $\mathbf{3} \cdot H_2O$ with 1,3-bis(triflyloxy)propane (98 mg, 0.288 mmol) to afford a dark purple solid: 82 mg, 53%; δ_H (500 MHz, CD_3CN) 8.57 (2 H, d, $J = 6.9$ Hz, C_5H_3N), 8.24 (2 H, s, C_5H_3N), 8.01 (2 H, d, $J = 6.6$ Hz, C_5H_3N), 7.86−7.80 (2 H, m, 2CH), 7.49 (4 H, d, $J = 8.5$ Hz, $2C_6H_4$), 7.36 (8 H, t, $J = 7.7$ Hz, Ph), 7.18−7.10 (16 H, Ph + 4CH), 6.96 (4 H, d, $J = 8.5$ Hz, $2C_6H_4$), 6.85 (2 H, d, $J = 15.8$ Hz, 2CH), 4.69−4.66 (2 H, m, NCH_2^{eq}), 4.29−4.20 (2 H, m, NCH_2^{ax}), 2.74−2.65 (2 H, m, CH_2). Anal. Calcd (%) for $C_{57}H_{48}F_{12}N_4P_2 \cdot 0.8H_2O$: C, 62.61; H, 4.57; N, 5.12. Found: C, 62.62; H, 4.56; N, 5.14. $m/z = 933.8$ ($[M - PF_6]^+$), 394.7 ($[M - 2PF_6]^{2+}$).

2.16. X-ray Crystallography. Crystals of the precursor compound Dpaca were obtained by slow evaporation of a dichloromethane solution at room temperature. Crystals of the salt $\mathbf{8} \cdot 0.5Et_2O \cdot 0.25MeCN$ were obtained by diffusion of diethyl ether vapor into an acetonitrile solution at room temperature, with the diffusion rate slowed by using a lid spiked with small holes. Data were collected on Oxford Diffraction XCalibur 2 or Bruker SMART APEX CCD X-ray diffractometers using MoK_α radiation ($\lambda = 0.71073$ Å), and processed by using the Oxford Diffraction CrysAlis RED[20] or Bruker SAINT[21] software packages.

TABLE 1: Crystallographic Data and Refinement Details for Dpaca and the Salt $\mathbf{8} \cdot 0.5Et_2O \cdot 0.25MeCN$

	Dpaca	$\mathbf{8} \cdot 0.5Et_2O \cdot 0.25MeCN$
formula	$C_{21}H_{17}NO$	$C_{38.5}H_{38.75}F_{12}N_{3.25}O_{0.5}P_2$
M	299.36	844.92
crystal system	monoclinic	triclinic
space group	$P2_1/c$	$P\bar{1}$
a, Å	8.966(1)	8.065(2)
b, Å	18.422(2)	13.810(3)
c, Å	10.485(2)	20.684(5)
α, deg	90.00	106.539(4)
β, deg	116.327(9)	99.424(4)
γ, deg	90.00	96.092(4)
V, Å^3	1552.1(3)	2150.1(9)
Z	4	2
D_{calcd} (Mg m^{-3})	1.281	1.305
T, K	100(2)	100(2)
μ, mm^{-1}	0.078	0.185
crystal size, mm^3	0.20 × 0.12 × 0.10	0.65 × 0.10 × 0.02
crystal appearance	yellow prism	brown needle
reflections collected	6708	8262
independent reflections (R_{int})	2727 (0.0436)	3865 (0.1129)
θ_{max}, deg (completeness)	25.08 (98.4%)	19.78 (99.5%)
reflections with $I > 2\sigma(I)$	1533	2157
goodness-of-fit on F^2	0.901	1.070
final $R1$, $wR2$ [$I > 2\sigma(I)$]	0.0362, 0.0476	0.0958, 0.2297
(all data)	0.0796, 0.0503	0.1690, 0.2637
peak and hole (e Å^{-3})	0.157, −0.167	0.676, −0.285

The structures were solved by direct methods using SIR-92[22] via WinGX,[23] or SHELXS-97,[24] and refined by full-matrix least-squares on all F_0^2 data using SHELXL-97.[25] All non-hydrogen atoms were refined anisotropically, except for the partially occupied solvent atoms in $\mathbf{8} \cdot 0.5Et_2O \cdot 0.25MeCN$. Hydrogen atoms were included in idealized positions by using the riding model, with thermal parameters of 1.2 times those of aromatic parent carbon atoms, and 1.5 times those of methyl parent carbons. For $\mathbf{8} \cdot 0.5Et_2O \cdot 0.25MeCN$, restraints were applied to the geometry of the solvent molecules and the data were cut at 1.05 Å since they were very weak beyond this resolution. All other calculations were carried out by using the SHELXTL package.[26] Crystallographic data and refinement details are presented in Table 1.

2.17. Hyper-Rayleigh Scattering. General details of the hyper-Rayleigh scattering (HRS) experiment have been discussed elsewhere,[27] and the experimental procedure and data analysis protocol for the femtosecond measurements used in this study were as previously described.[28] Measurements were carried out in acetonitrile, with crystal violet as an external octupolar reference ($\beta_{xxx,800} = 338 \times 10^{-30}$ esu in methanol),[28a] and local field correction factors at optical frequencies are applied to correct for the difference in solvent. All measurements were performed by using the 800 nm fundamental of a regenerative mode-locked Ti^{3+}:sapphire laser (Spectra Physics, model Tsunami, 100 fs pulses, 1 W, 80 MHz). Dilute solutions (10^{-4}−10^{-6} M) were used to ensure linear dependences of $I_{2\omega}/I_\omega^2$ on solute concentration, precluding the need for Lambert−Beer correction factors. The absence of frequency demodulation of the observed hyperpolarizability, that is, constant values of β versus amplitude modulation frequency, showed that no fluorescence contributions to the HRS signals were present at 400 nm. This situation may indicate: (i) a lack of fluorescence, (ii) spectral filtering out of fluorescence, or (iii) the fluorescence lifetime is too short for its demodulation to be observed within the bandwidth of the instrument. The reported β values are the averages taken from measurements at different amplitude modulation frequencies. HRS depolarization ratios ρ[29] were determined at 800 nm in acetonitrile according to a published methodology.[30] Although the precision of individual depolar-

ization measurements is high (fitting errors of ca. ± 0.02), multiple measurements on the crystal violet reference and on some of the samples indicated significant variability in the ρ values obtained. Hence, the errors for the whole data set have been estimated based on the variability of ca. ± 15% observed in the values obtained for the reference.

2.18. Stark Spectroscopy. The Stark apparatus, experimental methods and data collection procedure were as previously reported,[31] except that a Xe arc lamp was used as the light source in the place of a W filament bulb. The Stark spectrum for each compound was measured at least twice. Satisfactory fits of the Stark data for the salts **5**−**8** were obtained by using the observed absorption (ε/ν vs ν) spectra, but for **9**−**12** these spectra were modeled with a sum of three Gaussian curves that reproduce the data and separate the peaks. The first and second derivatives of the Gaussian curves were then used to fit the Stark spectra with Liptay's equation.[32] The dipole-moment change $\Delta\mu_{12} = \mu_e - \mu_g$ (where μ_e and μ_g are the excited and ground state dipole moments, respectively, associated with each of the optical transitions considered in the fit) was then calculated from the coefficient of the second derivative component. Butyronitrile was used as the glassing medium, for which the local field correction f_{int} is estimated as 1.33.[31] A two-state analysis of the ICT transitions gives

$$\Delta\mu_{ab}^2 = \Delta\mu_{12}^2 + 4\mu_{12}^2 \quad (1)$$

where $\Delta\mu_{ab}$ is the dipole-moment change between the diabatic states, and $\Delta\mu_{12}$ is the observed (adiabatic) dipole-moment change. The value of μ_{12} can be determined from the oscillator strength f_{os} of the transition by

$$|\mu_{12}| = \left(\frac{f_{os}}{1.08 \times 10^{-5} E_{max}}\right)^{1/2} \quad (2)$$

where E_{max} is the energy of the ICT maximum (in wavenumbers) and μ_{12} is in eÅ. The latter is converted into Debye units upon multiplying by 4.803. The degree of delocalization c_b^2 and electronic coupling matrix element H_{ab} for the diabatic states are given by

$$c_b^2 = \frac{1}{2}\left[1 - \left(\frac{\Delta\mu_{12}^2}{\Delta\mu_{12}^2 + 4\mu_{12}^2}\right)^{1/2}\right] \quad (3)$$

$$|H_{ab}| = \left|\frac{E_{max}(\mu_{12})}{\Delta\mu_{ab}}\right| \quad (4)$$

If the hyperpolarizability tensor β_0 has only nonzero elements along the CT direction, then this quantity is given by

$$\beta_0 = \frac{3\Delta\mu_{12}(\mu_{12})^2}{(E_{max})^2} \quad (5)$$

A relative error of ±20% is estimated for the β_0 values derived from the Stark data and using eq 5, while experimental errors of ±10% are estimated for μ_{12}, $\Delta\mu_{12}$ and $\Delta\mu_{ab}$, ±15% for H_{ab} and ±50% for c_b^2. Note that the ±20% uncertainty for the β_0 values is merely statistical and does not account for any errors introduced by two-state extrapolation.

2.19. Z-Scan Measurements. All compounds were investigated as DMF solutions placed in 1 mm path length glass cells. Measurements[33] were recorded by using a Clark MXR CPA-2001 Ti^{3+}:sapphire amplifier pumping a tunable Light Conversion TOPAS optical parametric amplifier (150 fs pulses, operated at 250 Hz repetition rate). The experiments were carried out at a number of wavelengths in the range 520−1600 nm. To obtain the relevant wavelengths, the optical parametric amplifier was appropriately tuned and one of the following modes of output was selected: idler-pump mixing, signal doubling, idler doubling, or the signal. The unwanted components of the TOPAS output were discarded through the use of polarizing optics, color glass filters, and spatial filtering. Other experimental details and the data processing procedure were as described previously.[34] The real and imaginary parts of γ of the solutes were computed assuming additivity of the nonlinear contributions of the solvent and the solute and the applicability of the Lorentz local field approximation. The errors on the γ values were estimated from the assessed accuracies of the parameters for the fitting of Z-scans for the solutions and the corresponding scans for the solvent. The nonlinear absorption, related to the imaginary part of γ, was also expressed in terms of the values of the two-photon absorption cross-section σ_2 calculated as shown previously.[34]

3. Results and Discussion

3.1. Synthesis and Characterization. The new DQ^{2+}-based chromophores (Figure 1) were prepared and isolated as their PF_6^- salts **5**−**12** following reactions between the appropriate 2,2′-bipyridyl (bpy) derivative and 1,2-bis(triflyloxy)ethane or 1,3-bis(triflyloxy)propane.[19] The required precursors **1**−**4** (Figure 1) were prepared in high yields via Wadsworth−Emmons reactions between 4-(diphenylamino)benzaldehyde or Dpaca and 4-[(diethoxyphosphinyl)methyl]-4′-methyl-2,2′-bipyridyl[17] or 4,4′-bis-[(diethoxyphosphinyl)methyl]-2,2′-bipyridyl.[18] A recently published synthesis of Dpaca involves a Vilsmeier reaction of 4-(diphenylamino)styrene,[35] with a yield ca. 10% lower than that we have achieved by using a Wittig oxopropenylation with (1,3-dioxolan-2-yl-methyl)tributyl phosphonium bromide.[36] Nickel et al. have reported using a method similar to ours, but with only 1.1 equivalents of the Wittig reagent and potassium *tert*-butoxide as the base instead of sodium hydride, resulting in a yield of 72%.[37]

The compound 4,4′-bis[(*E*)-2-(4-diphenylaminophenyl)ethenyl]-2,2′-bipyridyl (**3**) has been prepared previously via a PPh_3-derived Wittig reagent, but the isolated yield was only 50%.[38] Although we have previously used Knoevenagel-type condensations to synthesize related compounds containing Dmap or Jd π-ED groups,[15] such an approach is ineffective for the Dpap-substituted chromophores in **5**−**12**. Most of the products were isolated in pure form simply via reprecipitation, with yields in the range ca. 40−60%. However, column chromatographic purification was required in order to obtain satisfactory results for **6** and **10**, returning yields about half those for the other salts. All of the new compounds show diagnostic ^{1}H NMR spectra, and CHN elemental analyses provide further confirmation of identity and purity. In addition, informative +electrospray mass spectra were obtained, with the exceptions of the precursor compounds **3** and **4**.

3.2. Electronic Spectroscopy Studies. The UV−vis absorption spectra of salts **5**−**12** have been measured in acetonitrile and the results are presented in Table 2. These spectra are dominated by intense, low-energy bands in the visible region attributable to $\pi \rightarrow \pi^*$ intramolecular charge-transfer (ICT)

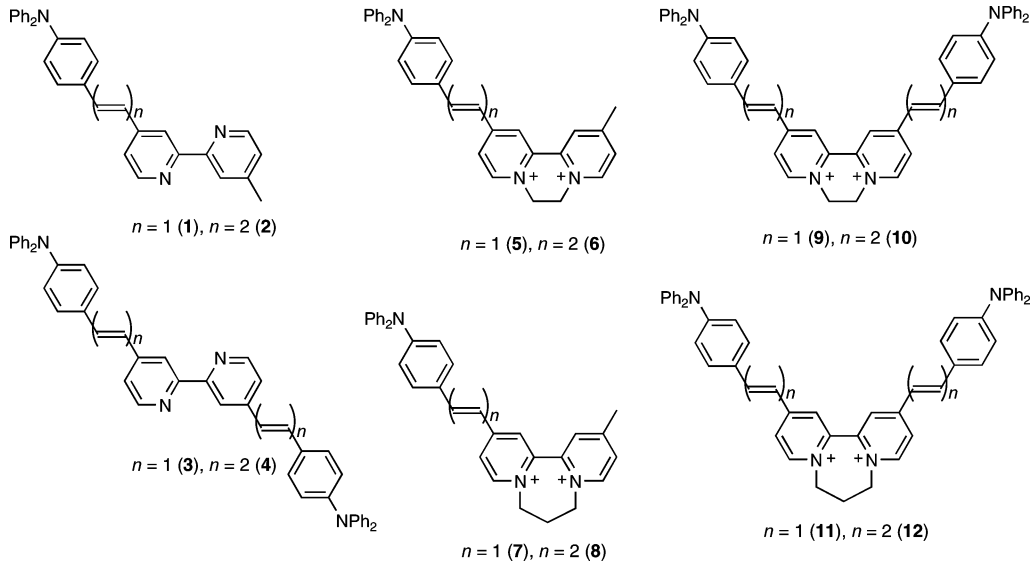

Figure 1. Chemical structures of the precursor compounds and DQ^{2+} derivatives prepared; the latter were isolated and studied as their PF_6^- salts. Shorthand: EDQ^{2+} = ethylene diquat; PDQ^{2+} = propylene diquat.

TABLE 2: UV-Vis Absorption and Electrochemical Data for Compounds 1−12 in Acetonitrile[a]

				E, V vs Ag−AgCl (ΔE_p, mV)[b]	
compound	λ_{max}, nm (ε, 10^3 M^{-1} cm^{-1})[a]	E_{max} (eV)	assignment	oxidations	reductions
1	389 (31.6)	3.19	ICT		
	290 (30.9)	4.28	$\pi \rightarrow \pi^*$		
2	404 (37.2)	3.07	ICT		
	302 (32.1)	4.11	$\pi \rightarrow \pi^*$		
3	395 (66.0)	3.14	ICT		
	299 (49.3)	4.15	$\pi \rightarrow \pi^*$		
4	410 (79.8)	3.02	ICT		
	316 (61.6)	3.92	$\pi \rightarrow \pi^*$		
5	551 (35.7)	2.25	ICT-1	1.05 (120)	−0.39 (90)
	394 (12.4)	3.15	ICT-2		−0.82 (90)
	302 (28.5)	4.11	$\pi \rightarrow \pi^*$		
6	568 (37.7)	2.18	ICT-1	1.00[c]	−0.38 (80)
	396 (20.8)	3.13	ICT-2		−0.81 (80)
	305 (31.6)	4.07	$\pi \rightarrow \pi^*$		
7	528 (42.0)	2.35	ICT-1	1.08 (100)	−0.55 (110)
	332 (14.0)	3.73	$\pi \rightarrow \pi^*$		−0.86 (100)
	287 (27.9)	4.32	$\pi \rightarrow \pi^*$		−1.26[d]
8	545 (41.6)	2.28	ICT-1	0.99 (100)	−0.53 (110)
	377 (17.5)	3.29	ICT-2		−0.84 (100)
	292 (24.4)	4.25	$\pi \rightarrow \pi^*$		−1.20[d]
9	551 (59.1)	2.25	ICT-1	1.03 (150)	−0.38 (80)
	426 (30.5)	2.91	ICT-2		−0.73 (80)
	298 (42.0)	4.16	$\pi \rightarrow \pi^*$		
10	571 (52.0)	2.17	ICT-1	0.94 (140)	−0.33 (80)
	426 (34.2)	2.91	ICT-2		−0.70 (90)
	306 (37.9)	4.05	$\pi \rightarrow \pi^*$		
11	527 (62.1)	2.35	ICT-1	1.07 (130)	−0.51 (120)
	339 (25.2)	3.66	$\pi \rightarrow \pi^*$		−0.78 (110)
	297 (41.4)	4.18	$\pi \rightarrow \pi^*$		
12	542 (55.9)	2.29	ICT-1	0.98 (140)	−0.48 (110)
	382 (32.1)	3.25	ICT-2		−0.76 (120)
	302 (43.2)	4.11	$\pi \rightarrow \pi^*$		

[a] Solutions ca. $2-3 \times 10^{-5}$ M. [b] Solutions ca. 10^{-3} M in analyte and 0.1 M in $[N(C_4H_9\text{-}n)_4]PF_6$ at a 2 mm disk glassy carbon working electrode with a scan rate of 200 mV s^{-1}. $E_{1/2}$ values are quoted unless stated otherwise. Ferrocene internal reference $E_{1/2}$ = 0.46 V, ΔE_p = 80−90 mV. [c] E_{pa} for an irreversible oxidation process. [d] E_{pc} for an irreversible reduction process.

excitations from the Dpap π-ED groups to the DQ^{2+} acceptors, denoted ICT-1. Weaker bands ascribed to other $\pi \rightarrow \pi^*$ transitions with little or no ICT character are also observed at higher energies. Bands with intermediate energies are (somewhat arbitrarily) denoted as being ICT in nature (i.e., ICT-2) if their maxima lie at wavelengths below about 380 nm, but of course the extent of charge-transfer character in a $\pi \rightarrow \pi^*$ transition is not simply a predictable function of its energy. Representative UV−vis spectra of **6**, **9**, **10**, and **11** are shown in Figure 2.

The ICT energies E_{max} of the neutral precursor compounds decrease both on extending the π-conjugated bridges (by 0.12 eV) and on moving from a monosubstituted (MS) species to its

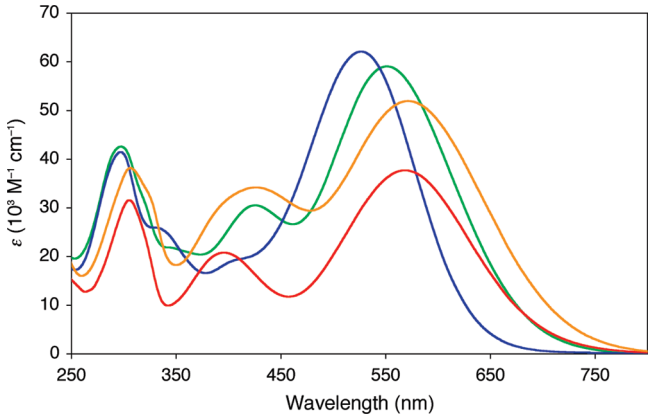

Figure 2. UV−vis absorption spectra of **6** (red), **9** (green), **10** (orange), and **11** (blue) at 293 K in acetonitrile.

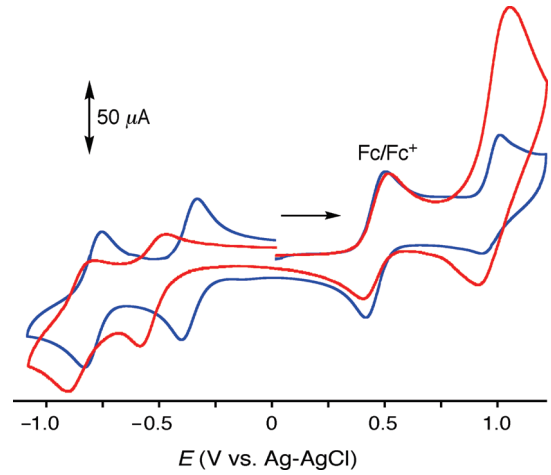

Figure 3. Cyclic voltammograms for the salts **6** (blue) and **8** (red) recorded at 200 mV s^{-1} in acetonitrile with a glassy carbon working electrode (Fc = ferrocene). The arrow indicates the direction of the initial scans.

disubstituted (DS) counterpart (by 0.05 eV). The E_{max} values of the other new chromophores display trends that we have observed previously in both DQ^{2+}-based chromophores[15b] and simpler monocationic pseudolinear species.[39] Thus, moving from an EDQ^{2+} chromophore to its PDQ^{2+} analogue causes blue-shifts of the ICT bands (as shown for **9** and **11** in Figure 2); for the dominant ICT-1 bands, the increase in E_{max} is almost constant at ca. 0.1 eV, but generally rather larger and more variable shifts are observed for the ICT-2 bands. This trend is due to the weaker electron-accepting strength of a PDQ^{2+} vs a EDQ^{2+} group, as shown electrochemically.[15b,40] On moving from a MS compound to its DS counterpart, E_{max}[ICT-1] remains essentially constant (as shown for **6** and **10** in Figure 2). In contrast, the ICT-2 bands show significant red shifts of ca. 0.2 eV for the EDQ^{2+} chromophores and smaller decreases (ca. 0.05 eV) for the PDQ^{2+} species. Notably, our previous studies with Dmap or Jd-substituted diquats revealed small *increases* in E_{max}[ICT-1] on moving from MS to DS chromophores.[15b] Moving from $n = 1$ to 2 causes E_{max}[ICT-1] to decrease by 0.06−0.08 eV.

A π-ED strength order of Dpap < Dmap < Jd has been derived by Kwon et al,[41] by using density functional theory (DFT)-calculated bond distances and ^{13}C NMR chemical shifts. This order is supported by the ICT energies of **5**−**12**, which are higher than those of the Dmap/Jd-substituted diquats we reported previously.[15b] For the ICT-1 band, respective red-shifts of 0.03−0.11 and 0.23−0.36 eV are observed on replacing Dpap with Dmap or Jd. The accompanying decreases in E_{max}[ICT-2] are even larger (as much as ca. 0.6 eV) for the EDQ^{2+} species, but we did not assign such bands in the Dmap/Jd-substituted PDQ^{2+} chromophores.[15b]

Several trends are also observed in the molar extinction coefficients ε of the lowest energy ICT bands. For the neutral precursor compounds, moving from $n = 1$ to 2 increases ε by ca. 20%, while the ε values for the DS species are about twice those of their MS counterparts. This latter trend is also found with the DQ^{2+} chromophores, but the increases in intensity are somewhat less than 2-fold (as shown for **6** and **10** in Figure 2). Small increases in ε are evident on moving from an EDQ^{2+} chromophore to its PDQ^{2+} analogue (as shown for **9** and **11** in Figure 2), contrasting with the more substantial changes accompanying this structural modification in Dmap/Jd-substituted diquats.[15b] Perhaps surprisingly, the ε values of these new DQ^{2+} species are not consistently affected by extending the π-conjugated bridges, showing either no significant change or small decreases.

3.3. Electrochemical Studies. We have investigated salts **5**−**12** by using cyclic voltammetry in acetonitrile, and the results are presented in Table 2. Representative voltammograms for **6** and **8** are shown in Figure 3. For each compound, waves with relatively large peak currents in the region ca. 1−1.1 V versus Ag−AgCl are attributable to oxidation of the Dpap units. Although our previous studies with Dmap/Jd-substituted diquats revealed only irreversible oxidations,[15b] return waves are observed for the Dpap-containing PDQ^{2+} species, and **8** even shows a quasireversible oxidation (although i_{pc} is somewhat smaller than i_{pa}; Figure 3). In keeping with the ICT energies (see above), the potentials for Dpap oxidation are always higher than those of their Dmap or Jd analogues;[15b] and the latter π-ED groups are hence easier to oxidize by ca. 0.1−0.2 and ca. 0.3−0.4 V, respectively. It is however notable that DFT-derived and photoelectron spectroscopy-measured ionization potentials follow the order Dmap > Jd > Dpap, implying that Dpap should be the most easily oxidized of these three π-ED units.[41]

Moving from an EDQ^{2+} chromophore to its PDQ^{2+} analogue does not affect the potentials of the oxidation processes significantly. The differences between the related MS and DS chromophores are also negligible, and both of these observations also apply to Dmap/Jd-substituted diquats.[15b] Moving from $n = 1$ to 2 causes E_{pa} or $E_{1/2}$ to decrease by ca. 100 mV, attributable to the increased electron-donating ability of (*E*,*E*)-buta-1,3-dienylene vs ethenylene units. The fact that somewhat larger corresponding changes of 150−200 mV are observed for the Dmap/Jd-substituted species[15b] indicates that this effect is more significant when stronger terminal π-EDs are present.

Each of salts **5**−**12** also shows two reversible or quasireversible one-electron reduction waves (Figure 3), and a third, irreversible wave below −1 V versus Ag−AgCl is detectable for **7** and **8**. The $E_{1/2}$ values for these reductions are slightly higher (by up to 140 mV) than those of the Dmap/Jd-substituted species,[15b] indicating that the DQ^{2+} units in the new compounds are reduced more easily. This trend is consistent with the less strongly electron-donating Dpap group(s) causing the diquats to be more electron-deficient when compared with those previously reported. Moving from $n = 1$ to 2 causes no change or very small increases in the $E_{1/2}$ values, while slightly larger increases (up to 110 mV for the second wave) are observed on moving from a MS compound to its DS analogue. The reductions become a little more favorable due to more effective electron delocalization in the larger π-conjugated systems. Previous electrochemical studies[40] (and the ICT energies

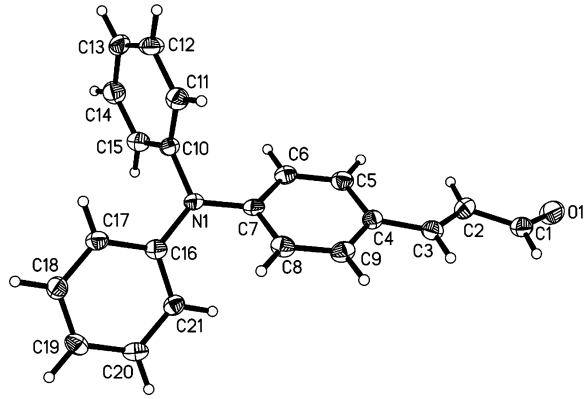

Figure 4. Representation of the molecular structure of Dpaca (50% probability ellipsoids).

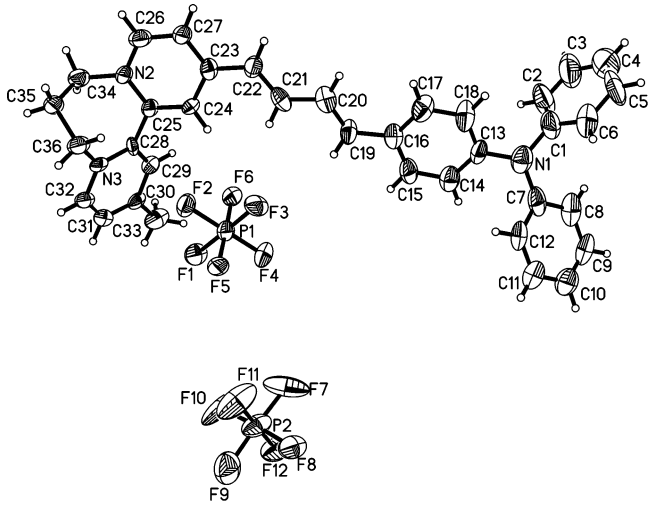

Figure 5. Representation of the molecular structure of the salt **8**·0.5Et_2O·0.25MeCN, with the solvent molecules removed for clarity (50% probability ellipsoids).

discussed above) show that a PDQ^{2+} unit is a weaker electron acceptor when compared with an EDQ^{2+} group, and replacing the latter with PDQ^{2+} hence causes the $E_{1/2}$ values to decrease (Figure 3). The observed cathodic shifts are larger for the first wave (130−160 mV) than for the second one (30−60 mV). All of these trends are also observed for the related Dmap/Jd-substituted species.[15b]

It is worth highlighting that the presence of reversible electrochemical behavior means that the new DQ^{2+} derivatives have potential for redox-switching of optical properties over multiple states. Redox-switching of NLO responses has been achieved previously with a range of transition metal complexes,[42] but not yet in any purely organic molecules.

3.4. Crystallographic Studies. This study is focused primarily on molecular electronic/optical properties, but bulk NLO properties that depend on macroscopic structures are relevant for potential applications. Although the new DQ^{2+} salts containing Dpap groups do not appear to crystallize as readily as their Dmap/Jd counterparts (for which nine single crystal X-ray structures have been obtained),[15b] we have solved the structure of the salt **8**·0.5Et_2O·0.25MeCN, together with that of its precursor aldehyde, Dpaca. Representations of the molecular structures are shown in Figures 4 and 5, and selected geometric parameters are collected in Table 3.

As for the acetone solvate of the analogous Dmap-containing compound,[15b] the salt **8**·0.5Et_2O·0.25MeCN crystallizes in the centrosymmetric space group $P\bar{1}$ and is therefore not expected to show bulk quadratic NLO effects. The geometric parameters of the cation in **8** are also generally similar to those of its Dmap counterpart **8′**,[15b] with the only notable exception being the N−C bond distance between the phenylene ring and the amino group. In **8′**, this distance is 1.366(3) Å, apparently ca. 0.05 Å shorter than that in **8** (1.413(15)). This observation is consistent with the stronger relative π-ED ability of the Dmap unit when compared with Dpap because it indicates that the amino group in the former is more strongly conjugated with the phenylene ring. Data obtained from other structural studies support this conclusion.[43] The dihedral angle between the two pyridyl rings in **8**·0.5Et_2O·0.25MeCN is ca. 52.4°, within the range found in other related structures.[15b,44]

TABLE 3: Selected Interatomic Distances and Angles for Dpaca and the Salt 8·0.5Et_2O·0.25MeCN

distance (Å)		distance (Å)		angle (deg)	
		Dpaca			
N1−C7	1.406(2)	C4−C5	1.396(2)	C2−C3−C4	129.43(16)
N1−C10	1.437(2)	C5−C6	1.384(2)	C1−C2−C3	119.73(16)
N1−C16	1.411(2)	C3−C4	1.448(2)	O1−C1−C2	126.44(16)
C6−C7	1.389(2)	C2−C3	1.328(2)		
C7−C8	1.394(2)	C1−C2	1.447(2)		
C8−C9	1.375(2)	O1−C1	1.216(2)		
C4−C9	1.384(2)				
		8·0.5Et_2O·0.25MeCN			
N1−C13	1.413(15)	N2−C25	1.354(13)	C16−C19−C20	128.9(13)
N1−C7	1.453(16)	N2−C26	1.351(14)	C19−C20−C21	122.4(12)
N1−C1	1.465(16)	C26−C27	1.364(15)	C20−C21−C22	128.3(12)
C13−C14	1.402(17)	C23−C27	1.375(14)	C21−C22−C23	124.4(11)
C14−C15	1.366(15)	C25−C28	1.493(15)		
C15−C16	1.390(16)	C28−C29	1.369(15)		
C16−C17	1.401(16)	C29−C30	1.397(15)		
C17−C18	1.377(16)	C30−C31	1.389(16)		
C13−C18	1.371(16)	C31−C32	1.369(16)		
C16−C19	1.457(16)	N3−C32	1.332(13)		
C19−C20	1.336(15)	N3−C28	1.381(13)		
C20−C21	1.438(16)	N3−C36	1.463(13)		
C21−C22	1.374(15)	C35−C36	1.529(13)		
C22−C23	1.436(15)	C34−C35	1.499(14)		
C23−C24	1.426(14)	N2−C34	1.482(13)		
C24−C25	1.339(14)				

TABLE 4: HRS Data and Depolarization Ratios for Salts 5−12 in Acetonitrile

	(10^{-30} esu)				(10^{-30} esu)	
salt	$\sqrt{\langle\beta^2_{HRS}\rangle}$[a]	β_0[b]	ρ[c]	k	β_{zzz}[d]	β_{zyy}[d]
5	330 ± 35	155 ± 15	3.7 ± 0.6		800 ± 80	
6	320 ± 32	160 ± 16	4.4 ± 0.7		770 ± 77	
7	310 ± 31	130 ± 13	2.5 ± 0.4		750 ± 75	
8	375 ± 37	170 ± 17	3.0 ± 0.5		900 ± 90	
9	325 ± 40	150 ± 18	3.5 ± 0.5	2	235 ± 30	470 ± 56
10	455 ± 45	230 ± 23	2.8 ± 0.4	6	120 ± 12	710 ± 71
11	385 ± 38	160 ± 16	2.8 ± 0.4	6	100 ± 10	615 ± 61
12	500 ± 50	225 ± 22	2.7 ± 0.4	8	100 ± 10	810 ± 81

[a] Orientationally averaged first hyperpolarizability without any assumption of symmetry or contributing tensor elements, measured by using an 800 nm Ti^{3+}:sapphire laser. The quoted cgs units (esu) can be converted into SI units (C^3 m^3 J^{-2}) by dividing by a factor of 2.693×10^{20}. [b] Static first hyperpolarizability estimated from $\sqrt{\langle\beta^2_{HRS}\rangle}$ via the two-state model.[46] [c] Depolarization ratio. [d] Hyperpolarizability tensor components derived from the HRS intensity and ρ measurements by using eqs 7−9.

The precursor Dpaca also crystallizes centrosymmetrically and shows geometric parameters similar to those of 4-(diphenylamino)benzaldehyde,[45] both having a trigonal planar N atom and effectively identical N−C(phenylene) distances (1.407(3) Å in 4-(diphenylamino)benzaldehyde). In both aldehydes, the shortening by up to ca. 0.3 Å of the latter distance with respect to the two N−C(phenyl) distances is consistent with stronger π-conjugation with the phenylene ring.

3.5. Hyper-Rayleigh Scattering Studies. We have measured the β values of salts **5**−**12** in acetonitrile solutions by using the HRS technique[27,28] with a 800 nm Ti^{3+}:sapphire laser and the results are shown in Table 4. This laser wavelength was chosen because the ICT-1 bands lie between 800 nm and the second harmonic (SH) at 400 nm (Figure 2). However, most of the chromophores do absorb relatively strongly at 400 nm, so the results obtained are strongly enhanced by resonance. Other available laser fundamentals, for example, 1064 or 1300 nm, would be unsuitable for most of the samples due to very strong absorption at their SH wavelengths. The hyperpolarizability data shown are orientationally averaged $\sqrt{\langle\beta^2_{HRS}\rangle}$ values derived from the total HRS intensity, regardless of molecular symmetry.

Although most of the compounds show an additional ICT-2 maximum to high energy of the main ICT-1 band and significant resonance enhancement also occurs, we have used the simple two-state model[46] and the major λ_{max} values (Table 2) to determine estimated β_0 values; the results are included in Table 4. It should be noted that this analysis is a major oversimplification because the DQ^{2+} derivatives, especially the DS ones, can not be accurately described as two-state systems. As observed previously with Dmap/Jd-substituted diquats,[15b] β_0 increases when moving from $n = 1$ to 2, although the difference for the pair **5**/**6** is not significant. The DS compounds show larger β_0 responses when compared with their MS counterparts, except for the pair **5**/**9**, and the related EDQ^{2+}/PDQ^{2+} pairs have indistinguishable β_0 values. However, these observations should be treated cautiously, given the number of approximations involved in deriving the data.

The electronic structures and thus hyperpolarizabilities of these chromophores are actually substantially 2D, and the main value of our HRS measurements is to assess the relative importance of different β tensor components. A C_{2v} symmetric chromophore has five nonzero β components, β_{zzz}, β_{zyy}, β_{zxx}, β_{yyz}, and β_{xxz}. Assuming Kleinman symmetry, $\beta_{zyy} = \beta_{yyz}$ and $\beta_{zxx} = \beta_{xxz}$, and if the structure is essentially 2D, then $\beta_{zxx} = \beta_{xxz} = 0$, so only β_{zzz} and β_{zyy} are significant. To determine "off-diagonal" tensor components, we have measured HRS depolarization ratios ρ for **5**−**12** and these are included in Table 4. The parameter ρ is the ratio of the intensities of the scattered SH light polarized parallel and perpendicular to the polarization direction of the fundamental beam.[29] A ρ value of 5 is the upper limit for purely dipolar symmetry, corresponding with a single dipolar β_{zzz} tensor component, and under ideal experimental conditions. Realistic conditions, such as using a condenser system to collect the SH light, will decrease the observed ρ value. The octupolar reference compound crystal violet gives a relatively low ρ value of 1.5.

The values of β_{zzz} and β_{zyy} can be determined from $\langle\beta^2_{HRS}\rangle$ and ρ as follows:

$$\left\{\langle\beta^2_{HRS}\rangle = \langle\beta^2_{ZZZ}\rangle + \langle\beta^2_{YZZ}\rangle\rho = \frac{\langle\beta^2_{ZZZ}\rangle}{\langle\beta^2_{YZZ}\rangle}\right. \quad (7)$$

The HRS intensities with parallel polarization for fundamental and SH wavelengths, $\langle\beta^2_{ZZZ}\rangle$, and for perpendicular polarization, $\langle\beta^2_{YZZ}\rangle$, are given in terms of the molecular tensor components β_{zzz} and β_{zyy} according to

$$\left\{\langle\beta^2_{ZZZ}\rangle = \frac{1}{7}\beta^2_{zzz} + \frac{6}{35}\beta_{zzz}\beta_{zyy} + \frac{9}{35}\beta^2_{zyy}\langle\beta^2_{YZZ}\rangle = \frac{1}{35}\beta^2_{zzz} - \frac{2}{105}\beta_{zzz}\beta_{zyy} + \frac{11}{105}\beta^2_{zyy}\right. \quad (8)$$

and ρ can be expressed in terms of the parameter $k = \beta_{zyy}/\beta_{zzz}$ by

$$\rho = \frac{15 + 18k + 27k^2}{3 - 2k + 11k^2} \quad (9)$$

Application of eqs 7−9 to our experimental data gives the β_{zzz} and β_{zyy} values shown in Table 4. Although eq 9 gives two solutions for k, the positive value has been used based on theoretical predictions; both finite field-DFT and coupled perturbed Hartree−Fock (CPHF) calculations predict that β_{zyy} dominates in DS DQ^{2+} derivatives.[15] Due to the uncertainties in the depolarization measurements, all k values are rounded to one significant figure.

Although the individual ρ values vary considerably, the average of 3.4 for the MS compounds **5**−**8**, together with their molecular structures, is consistent with the dominance of a single dipolar β_{zzz} tensor component. The DS chromophores in **9**−**12** give an average ρ value of 3.0, slightly lower than for their MS counterparts. Because the MS compounds are predominantly 1D dipoles, we have derived only their β_{zzz} responses. However, the average ρ value for the DS compounds, taken together with their molecular shapes, justify the derivation of β_{zyy} values. In each case, β_{zyy} dominates markedly over β_{zzz} (Table 4). In addition, β_{zyy} (but not β_{zzz}) increases on moving from $n = 1$ to 2. Given that the two types of chromophore are treated differently, assuming purely 1D dipolar symmetry ($C_{\infty v}$) for the MS species but essentially C_{2v} symmetry for the DS derivatives, comparing the β_{zzz} values for MS and DS pairs is inappropriate.

3.6. Stark Spectroscopic Studies. We have studied the salts **5**−**12** by using Stark spectroscopy[32] in butyronitrile glasses at 77 K, and the results are presented in Table 5. For the MS compounds, the single bands in the visible region were fitted satisfactorily. However, due to the presence of overlapped minor

TABLE 5: ICT Absorption and Stark Spectroscopic Data for Salts 5−12

salt	ν_{max}[a] (cm^{-1})	λ_{max}[a] (nm)	E_{max}[a] (eV)	f_{os}[b]	μ_{12}[c] (D)	$\Delta\mu_{12}$[d] (D)	$\Delta\mu_{ab}$[e] (D)	r_{12}[f] (Å)	r_{ab}[g] (Å)	c_b^2[h]	H_{ab}[i] (10^3 cm^{-1})	β_0[j] (10^{-30} esu)	$\Sigma\beta_0$ (10^{-30} esu)
5	18148	551	2.25	0.49	7.6	23.4	28.1	4.9	5.8	0.08	4.9	314	
6	17341	577	2.15	0.65	9.0	28.3	33.7	5.9	7.0	0.08	4.6	578	
7	18873	530	2.34	0.66	8.6	20.9	27.2	4.4	5.7	0.12	6.0	334	
8	18067	554	2.24	0.54	8.0	26.4	31.0	5.5	6.5	0.08	4.7	393	
9	(17502)	(571)	(2.17)	0.25	5.5	28.6	30.6	5.9	6.4	0.03	3.1	213	689
	18228 (18712)	549 (534)	2.26 (2.32)	0.61	8.3	23.2	28.6	4.8	6.0	0.09	5.4	350	
	22987 (22987)	435 (435)	2.85 (2.85)	0.35	5.7	27.0	29.4	5.6	6.1	0.04	4.4	127	
10	(16373)	(611)	(2.03)	0.17	4.7	33.0	34.3	6.9	7.2	0.02	2.2	204	876
	17341 (17744)	577 (564)	2.15 (2.20)	0.66	8.9	30.0	34.9	6.3	7.3	0.07	4.5	572	
	21979 (21979)	455 (455)	2.73 (2.73)	0.20	4.4	32.2	33.4	6.7	7.0	0.02	2.9	100	
11	(18309)	(546)	(2.27)	0.28	5.7	23.5	26.1	4.9	5.4	0.05	4.0	173	691
	18954 (19519)	528 (512)	2.35 (2.42)	0.73	8.9	24.3	30.1	5.1	6.3	0.10	5.8	385	
	23309 (23027)	429 (434)	2.89 (2.86)	0.35	5.7	28.8	31.0	6.0	6.5	0.03	4.2	133	
12	(17341)	(577)	(2.15)	0.24	5.4	25.9	28.1	5.4	5.9	0.04	3.3	192	735
	18067 (18712)	554 (534)	2.24 (2.32)	0.70	8.9	26.2	31.8	5.5	6.6	0.08	5.2	452	
	22342 (22019)	448 (454)	2.77 (2.73)	0.25	4.9	24.3	26.2	5.1	5.5	0.03	4.1	92	

[a] In butyronitrile at 77 K; observed absorption maxima, maxima for Gaussian fitting functions for **9**−**12** in brackets. The data in all subsequent columns relate to fitted curves if used. [b] For **5**−**8**, obtained from $(4.32 \times 10^{-9}$ M $cm^2)A$ where A is the numerically integrated area under the absorption peak; for **9**−**12**, obtained from $(4.60 \times 10^{-9}$ M $cm^2)\varepsilon_{max} \times fw_{1/2}$ where ε_{max} is the maximal molar extinction coefficient and $fw_{1/2}$ is the full width at half height (in wavenumbers). [c] Calculated using eq 2. [d] Calculated from $f_{int}\Delta\mu_{12}$ using $f_{int} = 1.33$. [e] Calculated from eq 1. [f] Delocalized electron-transfer distance calculated from $\Delta\mu_{12}/e$. [g] Effective (localized) electron-transfer distance calculated from $\Delta\mu_{ab}/e$. [h] Calculated from eq 3. [i] Calculated from eq 4. [j] Calculated from eq 5.

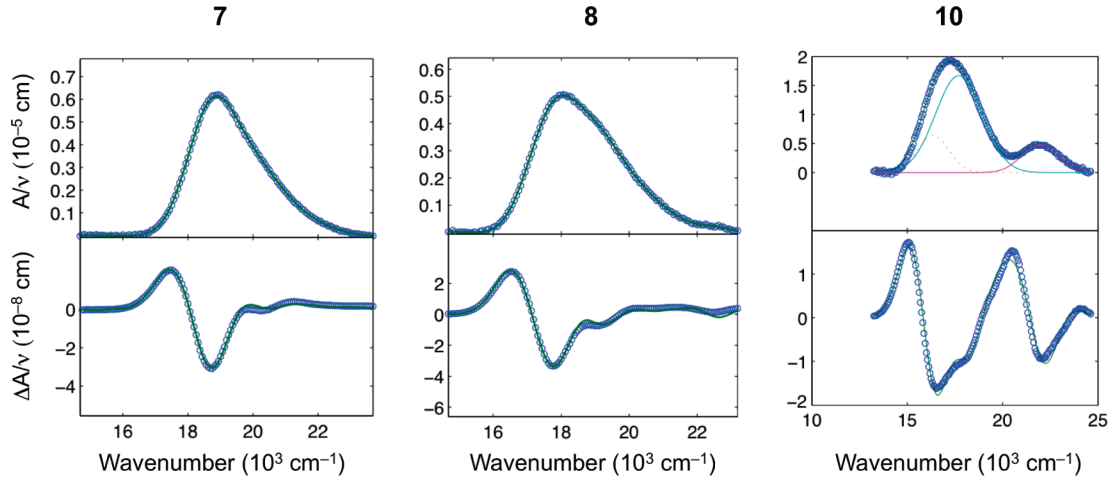

Figure 6. Stark spectra and calculated fits for **7**, **8**, and **10** in external electric fields of 3.57, 3.57, and 3.51×10^7 V m^{-1}, respectively. Top panel: absorption spectrum illustrating Gaussian curves used in data fitting for **10**; bottom panel: electroabsorption spectrum, experimental (blue) and fits (green) according to the Liptay equation.[32a]

bands to high energy, Gaussian-fitting of the absorption spectra with three curves was necessary to successfully model the Stark data for the DS compounds. Representative absorption and electroabsorption spectra for **7**, **8**, and **10** are shown in Figure 6, and the corresponding spectra for the other compounds are included in the Supporting Information (Figures S1 and S2).

The ICT bands of **5**−**12** show either no change or slight red shifts on moving from acetonitrile solutions to butyronitrile glasses (Tables 2 and 5). The ICT-1 bands do not shift significantly when $n = 1$, but decreases in their E_{max} values of 0.02−0.05 eV are observed for the compounds with $n = 2$. This behavior contrasts with that of the related Dmap/Jd-substituted species, which generally display small blue shifts on changing from solution to frozen glass (up to 0.07 eV).[15b] All of the ICT-1 E_{max} trends observed at room temperature are also found at 77 K, that is, decreases on moving from $n = 1$ to 2, increases on replacing EDQ^{2+} with PDQ^{2+}, and no difference between the related MS and DS species. The trends evident in the band intensities at 77 K (i.e., f_{os} and μ_{12}) generally agree with those already noted for ε at room temperature (see above). When analyzing these data for cases involving spectral deconvolution, the total values are used. Moving from $n = 1$ to 2 causes f_{os} and μ_{12} to decrease, except for the pair **5**/**6**. In every case, switching from a MS to the corresponding DS dication leads to marked increases in f_{os} and μ_{12}. Replacing EDQ^{2+} with PDQ^{2+} gives small increases in intensity, except for the pair **6**/**8**. It is worth noting that both of these exceptions (and the differences between **6** and **10**) imply that the intensities measured for **6** are higher than expected.

Because they are directly related to the chromophore length, the quantities $\Delta\mu_{12}$, $\Delta\mu_{ab}$, r_{12}, and r_{ab} should increase on moving from $n = 1$ to 2; such behavior is indeed observed (using averaged values for the DS compounds), except for the pair **11**/**12**. In similar manner, changing from a MS dication to its DS counterpart leads to modest increases in these parameters for all pairs except for **8**/**12**. Moving from an EDQ^{2+} chromophore to its PDQ^{2+} analogue is associated with small decreases in $\Delta\mu_{12}$, $\Delta\mu_{ab}$, r_{12}, and r_{ab}, but the relative change is much larger for **10** → **12**. Taken together, these observations

TABLE 6: Stark-Derived Total Static First Hyperpolarizabilities for Salts 5−12 and Their Dmap/Jd-Containing Analogues[a]

salt	β_0 (10^{-30} esu)	β_0[a] (10^{-30} esu)	β_0[b] (10^{-30} esu)
5	314	297	439
6	578	456	778
7	334	305	372
8	393	525	705
9	689	876	905
10	876	1173	1500
11	691	738	943
12	735	1126	1390

[a] All derived by using eq 5 with data measured in butyronitrile at 77 K. [b] Data for analogous Dmap-containing compound; taken from ref 15b. [c] Data for analogous Jd-containing compound; taken from ref 15b.

indicate that the dipole-moment changes determined for **12** are unexpectedly low.

D-A electronic coupling and orbital mixing are quantified by the parameters c_b^2 and H_{ab}, and these show the same trends as noted previously with Dmap/Jd-substituted diquats (again using averaged values for the DS compounds).[15b] Thus, moving from $n = 1$ to 2 causes decreases (or no significant change) in c_b^2 and H_{ab}; this is logical because π-orbital overlap diminishes over longer distances. The values of c_b^2 and H_{ab} also tend to decrease on moving from a MS chromophore to its DS analogue, and the EDQ^{2+} species have very similar or slightly smaller values when compared with their PDQ^{2+} counterparts.

Given that all of the observed visible absorption arises from ICT transitions, then even if deconvolution is used, each individual component can be adequately described as involving a ground and single excited state. It is hence reasonable to use the standard two-state model[46] (i.e., eq 5) to estimate β_0 values from the Stark data; the results are included in Table 5, and the sum totals of the β_0 responses associated with the three fitted Gaussian components are also quoted for **9**−**12**. In other related studies, we have demonstrated that using this approach generally affords total β_0 values similar to those obtained without spectral deconvolution.[39,47] The validity of, and assumptions involved in, applying this additive two-state approach to relatively complex systems have been discussed at length previously,[15b] but it is worth emphasizing that no other experimental method besides the clearly limited HRS exists for deriving β_0 values for chromophores of the type we report here.

The trends observed in the estimated β_0 values are in certain respects reminiscent of our previous studies with Dmap/Jd-substituted diquats.[15b] The only clear pattern for **5**−**12** is that moving from a MS chromophore to its DS analogue is associated with large increases in the quadratic NLO response, in the range ca. 50−120%. This effect is due largely to the strongly enhanced μ_{12} values for the DS chromophores (see above). Although extending the conjugated systems substantially increases β_0 in the Dmap/Jd-substituted species,[15b] the corresponding difference for the new compounds is only truly significant for the pair **5/6**. In keeping with our previous studies,[15b] the β_0 values for the EDQ^{2+} chromophores are similar to those of their PDQ^{2+} analogues.

Some comments regarding the performance of the new chromophores when compared with their Dmap/Jd-substituted counterparts are instructive. The collected data for these series of closely related compounds are shown in Table 6. The β_0 values of **5**−**12** are always smaller than those of their Jd analogues (but by highly variable proportions, ca. 10−90%), and in most cases smaller than (by up to ca. 50%), or similar to, those of their Dmap analogues. These observations are consistent with the established weaker π-ED ability of the Dpap group (see above). Nevertheless, the quadratic NLO responses of the new compounds are relatively impressive, with the largest (for **10**) approaching 10^{-27} esu. In all cases, the total β_0 response is considerably larger than that which we obtained for $[DAS]PF_6$ by using the same approach previously (236×10^{-30} esu).[48] Indeed, the total NLO responses estimated for the DS cations in the salts **9**−**12** are at least ca. 3-fold increased when compared with $[DAS]PF_6$. Therefore, polar materials containing these new symmetrical DQ^{2+} cations can be expected to show very large and 2D bulk quadratic NLO effects.

3.7. Two-Photon Absorption Studies. The salts **5**−**12** and their precursors **1**−**3** have been investigated in DMF solutions by using the Z-scan technique[33,34] at a number of laser wavelengths, to afford the dispersion of the real and imaginary parts of γ, the latter being also converted to the 2PA cross-sections σ_2. The results are collected in Table 7, and Figure 6 shows a representative set of data for **6**. Dispersion curves for all the other compounds are shown in Figures S3−S12 of the Supporting Information.

Examination of the data in Table 7 reveals several trends. First, since all of the investigated chromophores except for **3** are noncentrosymmetric, there is no condition disallowing one-photon absorption (1PA) reachable states to be populated also by 2PA. Therefore, it is to be expected that 2PA peaks will appear at wavelengths close to twice those of 1PA peaks, and this seems to be the case in general. The longest wavelength 2PA maximum for **1** and **2** is close to 700 nm, a little less than twice the wavelength of the first 1PA peak at ca. 400 nm. On the other hand, all of the salts **5**−**12** show 1PA at ca. 520−550 nm and their 2PA spectra show maxima at ca. 1100 nm for **5**−**10**, and at ca. 900 nm for **11** and **12** with a shoulder at ca. 1100 nm for the former. It is also worth noting that while the 1PA spectra for **1**−**3** show little variation between DMF and acetonitrile (Tables 2 and 7), the DQ^{2+} derivatives do display some solvatochromism. The ICT bands of the $n = 2$ species show blue shifts of ca. 0.1−0.2 eV on moving from acetonitrile to DMF solutions, while only negligible or very small changes are observed for the $n = 1$ compounds, except for **5**. However, it should be noted that higher concentrations were used for the DMF solutions, with 1 mm path length cells as opposed to 10 mm cells for the acetonitrile studies.

Trends are also evident in the magnitudes of the 2PA maxima. It is clear that the DQ^{2+} derivatives are much stronger two-photon absorbers (σ_2 values in the range of several hundred GM units) than their neutral precursors. Such behavior is not unexpected and may be understood in terms of the sum-over-states expressions that involve lower lying states in the case of the ionic species. It is worth noting that Zhou et al. used INDO/SOS calculations to derive σ_2 values of 454 GM at 918 nm and 182 GM at 729 nm for a chromophore analogous to $\mathbf{9}^{2+}$, but with $-NEt(C_2H_4OH)$ instead of $-NPh_2$ π-ED groups.[15] These values are of the same order of magnitude as those we have now measured. It is also to be expected that the magnitude of σ_2 may be affected by the extent of π-conjugation, that is, increased on moving from $n = 1$ to 2. However, this expectation is not generally confirmed by the data in Table 7. There is a strong enhancement of σ_2 when moving from **5** to **6**, and from **9** to **10**, but no difference between **7** and **8**, and even opposite trends for the pairs **1/2** and **11/12**. Even when taking into account possible experimental inaccuracies (ca. ± 20% for σ_2), these differences are significant. Therefore, it appears that the σ_2 values are also sensitive to other factors and that the degree

TABLE 7: Electronic Absorption and Cubic NLO Parameters for Compounds 1−3 and Salts 5−12 in DMF[a]

compound	$2\lambda_{max}$ (nm)	λ_{2ph}[b](nm)	σ_2[c](GM)	$\mathrm{Im}(\gamma)_{max}$[d]($10^{-33}$ esu)	$\mathrm{Re}(\gamma)_{ext}$[e]($10^{-33}$ esu)
1	778	740	63	0.21	0.29 (950 nm)
	580				
2	804	700	21	0.065	−0.35 (1000 nm)
	588				1.4 (850 nm)
3	790	740	180	0.63	−6.8 (850 nm)
	592				2.9 (650 nm)
5	1064	1190	260	2.3	14 (1370 nm)
	604	950	280	1.6	13 (850 nm)
6	1069	1190	670	6.1	24 (1190 nm)
	750	950	730	3.9	14 (900 nm)
7	1060	1130	310	2.5	12 (1370 nm)
	670	950	700	4.0	15 (810 nm)
8	1040	1130	340	2.8	21 (1190 nm)
	720				10 (900 nm)
9	1100	1130	280	2.3	5.6 (1280 nm)
	850	900	215	1.1	−7.5 (1060 nm)
10	1091	1130	550	4.5	3.2 (1370 nm)
	818				−8.4 (1000 nm)
11	1060	1130 (shoulder)	165	1.4	2.9 (1370 nm)
	670	950	240	1.4	−7.0 (1060 nm)
		620	−1840	−4.6	
12	1040	900	135	0.72	3.6 (1500 nm)
	744	770	350	1.3	−5.0 (850 nm)

[a] Unfortunately, compound **4** is insufficiently soluble to allow reliable determination of the NLO parameters. [b] 2PA maximum. [c] Maximum 2PA cross-section; note that negative values correspond with absorption bleaching rather than the usual 2PA. [d] Maximum of the imaginary part of γ. [e] Extrema of the real part of γ.

of π-conjugation is not always decisive. As noted above, moving from $n = 1$ to 2 leads to either no significant change or small decreases in the 1PA coefficient ε, so somewhat unintuitive behavior of σ_2 is hence not very surprising.

We note that the discussion of σ_2 values is equivalent to considering the imaginary part of γ, $\mathrm{Im}(\gamma)$. Comments on the dispersion of the real part of γ, $\mathrm{Re}(\gamma)$, can also be made, but only with caution due to inherently higher errors of determination of these parameters. In any case, the wavelength dependences of $\mathrm{Re}(\gamma)$ for all of the compounds appear rather complicated, with the γ values usually being positive at the long wavelength end of the measurement range and showing numerous features like extrema, changes of sign, etc., which typically coincide with the ranges of strong 2PA. It should be emphasized that the dispersion of $\mathrm{Re}(\gamma)$ may be quite complicated due to the presence of numerous terms in the perturbative expansion of the hyperpolarizability involving both one- and two-photon resonances,[49] and the understanding of experimental dispersion curves may therefore prove difficult.[50] Table 7 includes some of the extremal values of $\mathrm{Re}(\gamma)$ measured for **1**−**3** and **5**−**12**; as expected, the scaling of these follows roughly the scaling of the $\mathrm{Im}(\gamma)$ values.

Although our DQ^{2+} derivatives show some relatively high σ_2 values, especially considering that they are not very large molecules, it should be noted that various other chromophores, including transition metal complexes, possess much larger activities exceeding even 10^4 GM.[51] However, it is established that centrosymmetric systems do tend to give stronger 2PA when compared with similarly sized, related dipolar structures.[12k] The polar nature of DQ^{2+} derivatives that is essential to give nonzero values of β can therefore be expected to limit their potential for 2PA. Although we are not aware of any other experimental cubic NLO studies with DQ^{2+} derivatives, Xu et al. have recently reported Z-scan studies on *N*-methylpyridinium derivatives having two or three Dmap groups connected via ethylene bridges;[52] these compounds exhibit very strong saturable absorption when using picosecond pulses, and nanosecond pulses gave reverse saturable absorption in one case but saturable absorption for the other.

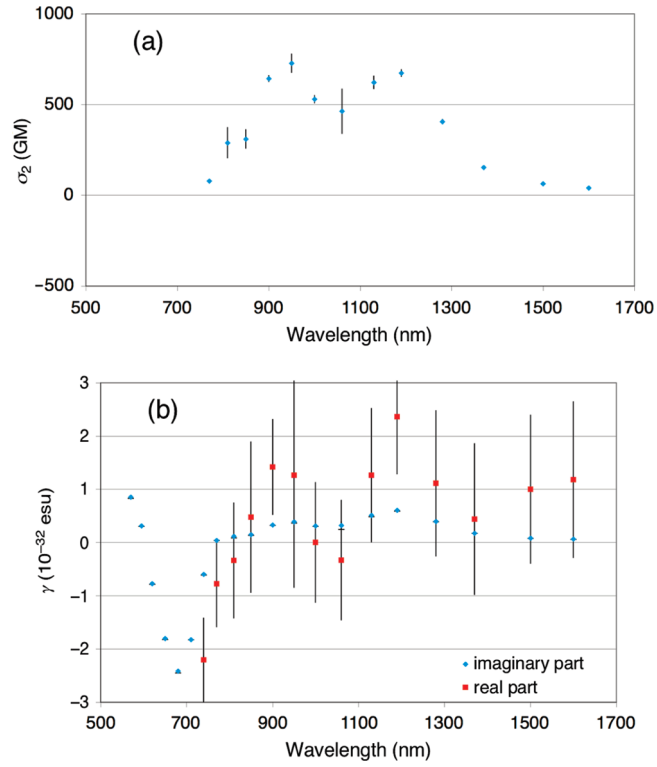

Figure 7. Dispersion of (a) the 2PA cross-section and (b) the complex cubic hyperpolarizability of salt **6**.

4. Conclusion

We have synthesized a family of new DQ^{2+}-based NLO chromophores containing one or two Dpap π-ED groups. Their visible absorption spectra are dominated by intense ICT bands that red shift on moving from $n = 1$ to 2 and blue shift on

extending the diquaternizing bridge ($EDQ^{2+} \rightarrow PDQ^{2+}$). Cyclic voltammograms show two reversible or quasireversible DQ^{2+}-based reductions and partially reversible Dpap oxidations. Single crystal X-ray structures have been determined for one PF_6^- salt and for the aldehyde precursor Dpaca, with both packing centrosymmetrically. HRS studies with a 800 nm laser show relatively large β responses, with depolarization measurements revealing dominant "off-diagonal" β_{zyy} tensor components for the DS compounds. Stark spectroscopy allows the estimation of β_0 values and shows that these do not differ significantly for the EDQ^{2+} and PDQ^{2+} pairs, but large increases occur on moving from a MS species to its DS counterpart. Z-scan measurements over a range of wavelengths reveal relatively high σ_2 values of up to 730 GM at 620 nm for one of the DS species. The new chromophores reported are therefore relatively rare in that they combine high quadratic and cubic NLO responses with potential redox-switchability in the absence of transition metal centers.

Acknowledgment. We thank the EPSRC for support (grants EP/E000738 and EP/D070732) and also the Fund for Scientific Research-Flanders (FWO-V, G.0312.08), the University of Leuven (GOA/2006/3), the NSF (grant CHE-0802907, "Powering the Planet: an NSF Center for Chemical Innovation"), and the Foundation for Polish Science. I. A. is a postdoctoral fellow of the FWO-V, and M. S. is a Laureate and J. O. is a Ph.D. scholar of the FNP Welcome programme.

Supporting Information Available: Crystallographic information in CIF format; Figures S1−S12 (PDF). This material is available free of charge via the Internet at http://pubs.acs.org.

References and Notes

(1) Śliwa, W.; Matusiak, G.; Bachowska, B. *Croat. Chem. Acta* **2006**, *79*, 513.

(2) (a) Yuan, C.-X.; Tao, X.-T.; Ren, Y.; Li, Y.; Yang, J.-X.; Yu, W.-T.; Wang, L.; Jiang, M.-H. *J. Phys. Chem. C* **2007**, *111*, 12811. (b) Yuan, C.-X.; Tao, X.-T.; Wang, L.; Yang, J.-X.; Jiang, M.-H. *J. Phys. Chem. C* **2009**, *113*, 6809.

(3) Kim, H. S.; Pham, T. T.; Yoon, K. B. *J. Am. Chem. Soc.* **2008**, *130*, 2134.

(4) Han, Z.-F.; Vaid, T. P.; Rheingold, A. L. *J. Org. Chem.* **2008**, *73*, 445.

(5) Xu, G.; Li, Y.; Zhou, W.-W.; Wang, G.-J.; Long, X.-F.; Cai, L.-Z.; Wang, M.-S.; Guo, G.-C.; Huang, J.-S.; Bator, G.; Jakubas, R. *J. Mater. Chem.* **2009**, *19*, 2179.

(6) Feng, S.-H.; Kim, Y. K.; Yang, S.-Q.; Chang, Y.-T. *Chem. Commun.* **2010**, *46*, 436.

(7) Selected general reviews:(a) *Molecular Nonlinear Optics: Materials, Physics and Devices*; Zyss, J.; Academic Press: Boston, 1994. (b) *Organic Nonlinear Optical Materials*; Bosshard, Ch., Sutter, K., Prêtre, Ph., Hulliger, J., Flörsheimer, M., Kaatz, P., Günter, P. Eds.; Advances in Nonlinear Optics, Vol. 1; Gordon & Breach: Amsterdam, The Netherlands, 1995. (c) *Nonlinear Optics of Organic Molecules and Polymers*; Nalwa, H. S., Miyata, S., Eds.; CRC Press: Boca Raton, FL, 1997. (d) Marder, S. R. *Chem. Commun.* **2006**, 131. (e) *Nonlinear Optical Properties of Matter: From Molecules to Condensed Phases*; Papadopoulos, M. G.; Leszczynski, J.; Sadlej, A. J., Eds.; Springer: Dordrecht, 2006. (f) Kuzyk, M. G. *J. Mater. Chem.* **2009**, *19*, 7444.

(8) Selected examples: (a) Marder, S. R.; Perry, J. W.; Schaefer, W. P. *Science* **1989**, *245*, 626. (b) Marder, S. R.; Perry, J. W.; Schaefer, W. P. *J. Mater. Chem.* **1992**, *2*, 985. (c) Marder, S. R.; Perry, J. W.; Yakymyshyn, C. P. *Chem. Mater.* **1994**, *6*, 1137. (d) Lee, O.-K.; Kim, K.-S. *Photonics Sci. News* **1999**, *4*, 9. (e) Sohma, S.; Takahashi, H.; Taniuchi, T.; Ito, H. *Chem. Phys.* **1999**, *245*, 359. (f) Kaino, T.; Cai, B.; Takayama, K. *Adv. Funct. Mater.* **2002**, *12*, 599. (g) Mohan Kumar, R.; Rajan Babu, D.; Ravi, G.; Jayavel, R. *J. Cryst. Growth* **2003**, *250*, 113. (h) Geis, W.; Sinta, R.; Mowers, W.; Deneault, S. J.; Marchant, M. F.; Krohn, K. E.; Spector, S. J.; Calawa, D. R.; Lyszczarz, T. M. *Appl. Phys. Lett.* **2004**, *84*, 3729. (i) Kuroyanagi, K.; Yanagi, K.; Sugita, A.; Hashimoto, H.; Takahashi, H.; Aoshima, S.-i.; Tsuchiya, Y. *J. Appl. Phys.* **2006**, *100*, 043117. (j) Liu, J.-J.; Merkt, F. *Appl. Phys. Lett.* **2008**, *93*, 131105. (k) Macchi, R.; Cariati, E.; Marinotto, D.; Roberto, D.; Tordin, E.; Ugo, R.; Bozio, R.; Cozzuol, M.; Pedron, D.; Mattei, G. *J. Mater. Chem.* **2010**, *20*, 1885.

(9) Selected examples: (a) Yitzchaik, S.; Marks, T. J. *Acc. Chem. Res.* **1996**, *29*, 197. (b) Alain, V.; Blanchard-Desce, M.; Ledoux-Rak, I.; Zyss, J. *Chem. Commun.* **2000**, 353. (c) Cariati, E.; Ugo, R.; Cariati, F.; Roberto, D.; Masciocchi, N.; Galli, S.; Sironi, A. *Adv. Mater.* **2001**, *13*, 1665. (d) Abbotto, A.; Beverina, L.; Bradamante, S.; Facchetti, A.; Klein, C.; Pagani, G. A.; Redi-Abshiro, M.; Wortmann, R. *Chem.—Eur. J.* **2003**, *9*, 1991. (e) Kim, H. S.; Lee, S. M.; Ha, K.; Jung, C.; Lee, Y.-J.; Chun, Y. S.; Kim, D.; Rhee, B. K.; Yoon, K. B. *J. Am. Chem. Soc.* **2004**, *126*, 673. (f) Yang, Z.; Aravazhi, S.; Schneider, A.; Seiler, P.; Jazbinšek, M.; Günter, P. *Adv. Funct. Mater.* **2005**, *15*, 1072. (g) Ruiz, B.; Yang, Z.; Gramlich, V.; Jazbinšek, M.; Günter, P. *J. Mater. Chem.* **2006**, *16*, 2839. (h) Kim, H. S.; Sohn, K. W.; Jeon, Y.; Min, H.; Kim, D.; Yoon, K. B. *Adv. Mater.* **2007**, *19*, 260. (i) Yang, Z.; Jazbinšek, M.; Ruiz, B.; Aravazhi, S.; Gramlich, V.; Günter, P. *Chem. Mater.* **2007**, *19*, 3512. (j) Morotti, T.; Calabrese, V.; Cavazzini, M.; Pedron, D.; Cozzuol, M.; Licciardello, A.; Tuccitto, N.; Quici, S. *Dalton Trans.* **2008**, 2974. (k) Figi, H.; Mutter, L.; Hunziker, C.; Jazbinšek, M.; Günter, P.; Coe, B. J. *J. Opt. Soc. Am. B* **2008**, *25*, 1786. (l) Compain, J.-D.; Mialane, P.; Dolbecq, A.; Marrot, J.; Proust, A.; Nakatani, K.; Yu, P.; Sécheresse, F. *Inorg. Chem.* **2009**, *48*, 6222.

(10) Selected examples: (a) Kawase, K.; Mizuno, M.; Sohma, S.; Takahashi, H.; Taniuchi, T.; Urata, Y.; Wada, S.; Tashiro, H.; Ito, H. *Opt. Lett.* **1999**, *24*, 1065. (b) Kawase, K.; Hatanaka, T.; Takahashi, H.; Nakamura, K.; Taniuchi, T.; Ito, H. *Opt. Lett.* **2000**, *25*, 1714. (c) Taniuchi, T.; Okada, S.; Nakanishi, H. *Appl. Phys. Lett.* **2004**, *95*, 5984. (d) Taniuchi, T.; Ikeda, S.; Okada, S.; Nakanishi, H. *Jap. J. Appl. Phys.* **2005**, *44*, L652. (e) Schneider, A.; Neis, M.; Stillhart, M.; Ruiz, B.; Khan, R. U. A.; Günter, P. *J. Opt. Soc. Am. B* **2006**, *23*, 1822. (f) Schneider, A.; Stillhart, M.; Günter, P. *Opt. Express* **2006**, *14*, 5376. (g) Yang, Z.; Mutter, L.; Stillhart, M.; Ruiz, B.; Aravazhi, S.; Jazbinšek, M.; Schneider, A.; Gramlich, V.; Günter, P. *Adv. Funct. Mater.* **2007**, *17*, 2018.

(11) (a) *Terahertz Sources and Systems*; Miles, R. E., Harrison, P., Lippens, D., Eds.; NATO Science Series II,; Kluwer: Dordrecht, 2001; Vol. 27. (b) Ferguson, B.; Zhang, X.-C. *Nat. Mater.* **2002**, *1*, 26. (c) McEntee, J. *Chem. World* **2007**, *March*, 52–56. (d) http://www.teraview.com, TeraView terahertz technology for 3D imaging and spectroscopy, accessed October 14, 2010.

(12) Selected examples: (a) Wang, C.; Wang, X.-M.; Shao, Z.-S.; Zhao, X.; Zhou, G.-Y.; Wang, D.; Fang, Q.; Jiang, M.-H. *Appl. Opt.* **2001**, *40*, 2475. (b) Zheng, Q.-D.; He, G. S.; Lin, T.-C.; Prasad, P. N. *J. Mater. Chem.* **2003**, *13*, 2499. (c) He, G. S.; Lin, T.-C.; Prasad, P. N.; Cho, C.-C.; Yu, L.-J. *Appl. Phys. Lett.* **2003**, *82*, 4717. (d) Yang, Z.; Wu, Z.-K.; Ma, J.-S.; Xia, A.-D.; Li, Q.-S.; Liu, C.-L.; Gong, Q.-H. *Appl. Phys. Lett.* **2005**, *86*, 061903. (e) Samoc, M.; Morrall, J. P.; Dalton, G. T.; Cifuentes, M. P.; Humphrey, M. G. *Angew. Chem., Int. Ed.* **2007**, *46*, 731. (f) Terenziani, F.; Katan, C.; Badaeva, E.; Tretiak, S.; Blanchard-Desce, M. *Adv. Mater.* **2008**, *20*, 4641. (g) Jana, A.; Jang, S. Y.; Shin, J.-Y.; De, A. K.; Goswami, D.; Kim, D.; Bharadwaj, P. J. *Chem.—Eur. J.* **2008**, *14*, 10628. (h) D'Aléo, A.; Picot, A.; Baldeck, P. L.; Andraud, C.; Maury, O. *Inorg. Chem.* **2008**, *47*, 10269. (i) He, G. S.; Tan, L.-S.; Zheng, Q.-D.; Prasad, P. N. *Chem. Rev.* **2008**, *108*, 1245. (j) Collings, J. C.; Poon, S.-Y.; Le Droumaguet, C.; Charlot, M.; Katan, C.; Pålsson, L.-O.; Beeby, A.; Mosely, J. A.; Kaiser, H. M.; Kaufmann, D.; Wong, W.-Y.; Blanchard-Desce, M.; Marder, T. B. *Chem.—Eur. J.* **2009**, *15*, 198. (k) Pawlicki, M.; Collins, H. A.; Denning, R. G.; Anderson, H. L. *Angew. Chem., Int. Ed.* **2009**, *48*, 3244. (l) Dvornikov, A. S.; Walker, E. P.; Rentzepis, P. M. *J. Phys. Chem. A* **2009**, *113*, 13633.

(13) Selected examples: (a) Wortmann, R.; Krämer, P.; Glania, C.; Lebus, S.; Detzer, N. *Chem. Phys.* **1993**, *173*, 99. (b) Moylan, C. R.; Ermer, S.; Lovejoy, S. M.; McComb, I.-H.; Leung, D. S.; Wortmann, R.; Krämer, P.; Twieg, R. J. *J. Am. Chem. Soc.* **1996**, *118*, 12950. (c) Di Bella, S.; Fragalà, I.; Ledoux, I.; Diaz-Garcia, M. A.; Marks, T. J. *J. Am. Chem. Soc.* **1997**, *119*, 9550. (d) Wolff, J. J.; Längle, D.; Hillenbrand, D.; Wortmann, R.; Matschiner, R.; Glania, C.; Krämer, P. *Adv. Mater.* **1997**, *9*, 138. (e) Averseng, F.; Lacroix, P. G.; Malfant, I.; Lenoble, G.; Cassoux, P.; Nakatani, K.; Maltey-Fanton, I.; Delaire, J. A.; Aukauloo, A. *Chem. Mater.* **1999**, *11*, 995. (f) Hilton, A.; Renouard, T.; Maury, O.; Le Bozec, H.; Ledoux, I.; Zyss, J. *Chem. Commun.* **1999**, 2521. (g) Lacroix, P. G. *Eur. J. Inorg. Chem.* **2001**, 339. (h) Ostroverkhov, V.; Petschek, R. G.; Singer, K. D.; Twieg, R. J. *Chem. Phys. Lett.* **2001**, *340*, 109. (i) Di Bella, S.; Fragalà, I.; Ledoux, I.; Zyss, J. *Chem.—Eur. J.* **2001**, *7*, 3738. (j) Yang, M.-L.; Champagne, B. *J. Phys. Chem. A* **2003**, *107*, 3942. (k) Wortmann, R.; Lebus-Henn, S.; Reis, H.; Papadopoulos, M. G. *J. Mol. Struct. (Theochem)* **2003**, *633*, 217. (l) Cui, Y.-Z.; Fang, Q.; Huang, Z.-L.; Xue, G.; Yu, W.-T.; Lei, H. *Opt. Mater.* **2005**, *27*, 1571. (m) Rigamonti, L.; Demartin, F.; Forni, A.; Righetto, S.; Pasini, A. *Inorg. Chem.* **2006**, *45*, 10976. (n) Li, H.-P.; Han, K.; Tang, G.; Shen, X.-P.; Wang, H.-T.; Huang, Z.-M.; Zhang, Z.-H.; Bai, L.; Wang, Z.-Y. *Chem. Phys. Lett.* **2007**, *444*, 80. (o) Zrig, S.; Koeckelberghs, G.; Verbiest, T.; Andrioletti, B.; Rose, E.; Persoons, A.; Asselberghs, I.; Clays, K. *J. Org. Chem.* **2007**, *72*, 5855. (p) Liu, C.-G.; Qiu, Y.-Q.; Su, Z.-M.; Yang, G.-C.; Sun, S.-L. *J. Phys. Chem. C* **2008**, *112*, 7021.

(14) Selected examples: (a) Verbiest, T.; Clays, K.; Samyn, C.; Wolff, J.; Reinhoudt, D.; Persoons, A. *J. Am. Chem. Soc.* **1994**, *116*, 9320. (b) Zyss, J.; Ledoux, I. *Chem. Rev.* **1994**, *94*, 77. (c) Dhenaut, C.; Ledoux, I.;

Samuel, I. D. W.; Zyss, J.; Bourgault, M.; Le Bozec, H. *Nature* **1995**, *374*, 339. (d) McDonagh, A. M.; Humphrey, M. G.; Samoc, M.; Luther-Davies, B.; Houbrechts, S.; Wada, T.; Sasabe, H.; Persoons, A. *J. Am. Chem. Soc.* **1999**, *121*, 1405. (e) Vance, F. W.; Hupp, J. T. *J. Am. Chem. Soc.* **1999**, *121*, 4047. (f) Wolff, J. J.; Siegler, F.; Matschiner, R.; Wortmann, R. *Angew. Chem., Int. Ed.* **2000**, *39*, 1436. (g) Cho, B. R.; Piao, M. J.; Son, K. H.; Lee, S. H.; Yoon, S. J.; Jeon, S.-J.; Cho, M.-H. *Chem.—Eur. J.* **2002**, *8*, 3907. (h) Le Bouder, T.; Maury, O.; Bondon, O.; Costuas, K.; Amouyal, E.; Ledoux, I.; Zyss, J.; Le Bozec, H. *J. Am. Chem. Soc.* **2003**, *125*, 12284. (i) Maury, O.; Viau, L.; Sénéchal, K.; Corre, B.; Guégan, J.-P.; Renouard, T.; Ledoux, I.; Zyss, J.; Le Bozec, H. *Chem.—Eur. J.* **2004**, *10*, 4454. (j) Maury, O.; Le Bozec, H. *Acc. Chem. Res.* **2005**, *38*, 691. (k) Coe, B. J.; Harris, J. A.; Brunschwig, B. S.; Asselberghs, I.; Clays, K.; Garín, J.; Orduna, J. *J. Am. Chem. Soc.* **2005**, *127*, 13399. (l) Le Floc'h, V.; Brasselet, S.; Zyss, J.; Cho, B. R.; Lee, S. H.; Jeon, S.-J.; Cho, M.-H.; Min, K. S.; Suh, M. P. *Adv. Mater.* **2005**, *17*, 196. (m) Hennrich, G.; Omenat, A.; Asselberghs, I.; Foerier, S.; Clays, K.; Verbiest, T.; Serrano, J. L. *Angew. Chem., Int. Ed.* **2006**, *45*, 4203. (n) Jeong, M.-Y.; Kim, H. M.; Jeon, S.-J.; Brasselet, S.; Cho, B. R. *Adv. Mater.* **2007**, *19*, 2107. (o) Liu, Y.; Xu, X.; Zheng, F.; Cui, Y. *Angew. Chem., Int. Ed.* **2008**, *47*, 4538. (p) Akdas-Kilig, H.; Roisnel, T.; Ledoux, I.; Le Bozec, H. *New J. Chem.* **2009**, *33*, 1470.

(15) (a) Coe, B. J.; Harris, J. A.; Brunschwig, B. S.; Garín, J.; Orduna, J. *J. Am. Chem. Soc.* **2005**, *127*, 3284. (b) Coe, B. J.; Fielden, J.; Foxon, S. P.; Harris, J. A.; Helliwell, M.; Brunschwig, B. S.; Asselberghs, I.; Clays, K.; Garín, J.; Orduna, J. *J. Am. Chem. Soc.* **2010**, *132*, 10498.

(16) Zhou, Y.-F.; Meng, F.-Q.; Zhao, X.; Feng, S.-Y.; Jiang, M.-H. *Chem. Phys.* **2001**, *269*, 441.

(17) Hartshorn, C. M.; Maxwell, K. A.; White, P. S.; DeSimone, J. M.; Meyer, T. J. *Inorg. Chem.* **2001**, *40*, 601.

(18) Gillaizeau-Gauthier, I.; Odobel, F.; Alebbi, M.; Argazzi, R.; Costa, E.; Bignozzi, C. A.; Qu, P.; Meyer, G. J. *Inorg. Chem.* **2001**, *40*, 6073.

(19) Lindner, E.; von Au, G.; Eberle, H.-J. *Chem. Ber.* **1981**, *114*, 810.

(20) *CrysAlis RED*, Version 1.171.32.29; Oxford Diffraction Ltd., Yarnton: Oxfordshire, United Kingdom, 2006.

(21) *SAINT*, Version 6.45; Bruker AXS Inc.: Madison, Wisconsin, USA, 2003.

(22) Altomare, A.; Cascarano, G.; Giacovazzo, C.; Guagliardi, A.; Burla, M. C.; Polidori, G.; Camalli, M. *J. Appl. Crystallogr.* **1994**, *27*, 435.

(23) Farrugia, L. J. *J. Appl. Crystallogr.* **1999**, *32*, 837.

(24) Sheldrick, G. M. *Acta Crystallogr., Sect. A* **1990**, *46*, 467.

(25) Sheldrick, G. M. *SHELXS 97: Programs for Crystal Structure Analysis*, Release 97−2; University of Göttingen: Göttingen, Germany, 1997.

(26) *SHELXTL*, Version 6.10; Bruker AXS Inc.: Madison, Wisconsin, USA, 2000.

(27) (a) Clays, K.; Persoons, A. *Phys. Rev. Lett.* **1991**, *66*, 2980. (b) Clays, K.; Persoons, A. *Rev. Sci. Instrum.* **1992**, *63*, 3285. (c) Hendrickx, E.; Clays, K.; Persoons, A. *Acc. Chem. Res.* **1998**, *31*, 675.

(28) (a) Olbrechts, G.; Strobbe, R.; Clays, K.; Persoons, A. *Rev. Sci. Instrum.* **1998**, *69*, 2233. (b) Olbrechts, G.; Wostyn, K.; Clays, K.; Persoons, A. *Opt. Lett.* **1999**, *24*, 699923-1. (c) Clays, K.; Wostyn, K.; Olbrechts, G.; Persoons, A.; Watanabe, A.; Nogi, K.; Duan, X.-M.; Okada, S.; Oikawa, H.; Nakanishi, H.; Vogel, H.; Beljonne, D.; Brédas, J.-L. *J. Opt. Soc. Am. B* **2000**, *17*, 256. (d) Franz, E.; Harper, E. C.; Coe, B. J.; Zahradnik, P.; Clays, K.; Asselberghs, I. *Proc. SPIE-Int. Soc. Opt. Eng.* **2008**, *6999*, 699923.

(29) Heesink, G. J. T.; Ruiter, A. G. T.; van Hulst, N. F.; Bölger, B. *Phys. Rev. Lett.* **1993**, *71*, 999.

(30) (a) Hendrickx, E.; Boutton, C.; Clays, K.; Persoons, A.; van Es, S.; Biemans, T.; Meijer, B. *Chem. Phys. Lett.* **1997**, *270*, 241. (b) Boutton, C.; Clays, K.; Persoons, A.; Wada, T.; Sasabe, H. *Chem. Phys. Lett.* **1998**, *286*, 101.

(31) (a) Shin, Y. K.; Brunschwig, B. S.; Creutz, C.; Sutin, N. *J. Phys. Chem.* **1996**, *100*, 8157. (b) Coe, B. J.; Harris, J. A.; Brunschwig, B. S. *J. Phys. Chem. A* **2002**, *106*, 897.

(32) (a) Liptay, W. In *Excited States*; Lim, E. C., Ed.; Academic Press: New York, 1974; Vol. 1, pp 129−229. (b) Bublitz, G. U.; Boxer, S. G. *Annu. Rev. Phys. Chem.* **1997**, *48*, 213. (c) Vance, F. W.; Williams, R. D.; Hupp, J. T. *Int. Rev. Phys. Chem.* **1998**, *17*, 307. (d) Brunschwig, B. S.; Creutz, C.; Sutin, N. *Coord. Chem. Rev.* **1998**, *177*, 61.

(33) (a) Sheik-Bahae, M.; Said, A. A.; van Stryland, E. W. *Opt. Lett.* **1989**, *14*, 955. (b) Sheik-Bahae, M.; Said, A. A.; Wei, T. H.; Hagan, D. J.; van Stryland, E. W. *IEEE J. Quantum Electron.* **1990**, *26*, 760. (c) van Stryland, E. W.; Sheik-Bahae, M. *Opt. Eng.* **1998**, *60*, 655.

(34) Samoc, M.; Samoc, A.; Dalton, G. T.; Cifuentes, M. P.; Humphrey, M. G.; Fleitz, P. A. In *Multiphoton Processes in Organics and Their Application*; Rau, I.; Kajzar, F., Eds.; Old City Publishing: Philadelphia, 2010, in press.

(35) Liang, M.; Xu, W.; Cai, F.-S.; Chen, P.-Q.; Peng, B.; Chen, J.; Li, Z.-M. *J. Phys. Chem. C* **2007**, *111*, 4465.

(36) Spangler, C. W.; McCoy, R. K. *Synth. Commun.* **1988**, *18*, 51.

(37) Nickel, E.; Spangler, C. W.; Rebane, A. Porphyrins with enhanced multi-photon absorption cross-sections for photodynamic therapy, U.S. Pat. 6,953,570, 2005.

(38) Karthikeyan, C S.; Thelakkat, M. *Inorg. Chim. Acta* **2008**, *361*, 635.

(39) Coe, B. J.; Foxon, S. P.; Harper, E. C.; Harris, J. A.; Helliwell, M.; Raftery, J.; Asselberghs, I.; Clays, K.; Franz, E.; Brunschwig, B. S.; Fitch, A. G. *Dyes Pigments* **2009**, *82*, 171.

(40) Kuzuya, M.; Kondo, S.-I.; Murase, K. *J. Phys. Chem.* **1993**, *97*, 7800.

(41) Kwon, O.; Barlow, S.; Odom, S. A.; Beverina, L.; Thompson, N. J.; Zojer, E.; Brédas, J.-L.; Marder, S. R. *J. Phys. Chem. A* **2005**, *109*, 9346.

(42) Selected examples: (a) Coe, B. J.; Houbrechts, S.; Asselberghs, I.; Persoons, A. *Angew. Chem., Int. Ed.* **1999**, *38*, 366. (b) Weyland, T.; Ledoux, I.; Brasselet, S.; Zyss, J.; Lapinte, C. *Organometallics* **2000**, *19*, 5235. (c) Malaun, M.; Reeves, Z. R.; Paul, R. L.; Jeffery, J. C.; McCleverty, J. A.; Ward, M. D.; Asselberghs, I.; Clays, K.; Persoons, A. *Chem. Commun.* **2001**, 49. (d) Powell, C. E.; Cifuentes, M. P.; Morrall, J. P.; Stranger, R.; Humphrey, M. G.; Samoc, M.; Luther-Davies, B.; Heath, G. A. *J. Am. Chem. Soc.* **2003**, *125*, 602. (e) Sporer, C.; Ratera, I.; Ruiz-Molina, D.; Zhao, Y.-X.; Vidal-Gancedo, J.; Wurst, K.; Jaitner, P.; Clays, K.; Persoons, A.; Rovira, C.; Veciana, J. *Angew. Chem., Int. Ed.* **2004**, *43*, 5266. (f) Cifuentes, M. P.; Powell, C. E.; Morrall, J. P.; McDonagh, A. M.; Lucas, N. T.; Humphrey, M. G.; Samoc, M.; Houbrechts, S.; Asselberghs, I.; Clays, K.; Persoons, A.; Isoshima, T. *J. Am. Chem. Soc.* **2006**, *128*, 10819. (g) Boubekeur-Lecaque, L.; Coe, B. J.; Clays, K.; Foerier, S.; Verbiest, T.; Asselberghs, I. *J. Am. Chem. Soc.* **2008**, *130*, 3286.

(43) The structure of the Jd-containing salt (*E*)-*N*-methyl-4-[2-(2,3,6,7-tetrahydro-1*H*,5*H*-pyrido[3,2,1-*ij*]quinolin-9-yl)ethenyl]pyridinium hexafluorophosphate is described partially in ref 39 and the average of the N(amino)−C(phenylene) distances for the two independent cations in the unit cell is 1.371(7) Å. We have also obtained a structure for (*E*)-*N*-methyl-4-[2-(4-diphenylaminophenyl)ethenyl]pyridinium hexafluorophosphate (Coe, B. J.; Helliwell, M.; Silverman, A. B., unpublished results) and this shows a N(amino)−C(phenylene) distance of 1.429(2) Å, clearly significantly longer than that in its Jd analogue and consistent with the stronger π-ED ability of Jd when compared with Dpap.

(44) (a) Mori, Y.; Matsuyama, Y.; Yamada, S.; Maeda, K. *Acta Crystallogr., Sect. C* **1992**, *48*, 894. (b) Knoch, F.; Smauch, G.; Kisch, H. *Z. Kristallogr.* **1995**, *210*, 225.

(45) Wang, H.-L.; Xu, W.-Y.; Zhang, B.; Xiao, W.-J.; Wu, H. *Acta Crystallogr., Sect. E* **2009**, *65*, o149.

(46) (a) Oudar, J. L.; Chemla, D. S. *J. Chem. Phys.* **1977**, *66*, 2664. (b) Oudar, J. L. *J. Chem. Phys.* **1977**, *67*, 446.

(47) Coe, B. J.; Foxon, S. P.; Harper, E. C.; Helliwell, M.; Raftery, J.; Swanson, C. A.; Brunschwig, B. S.; Clays, K.; Franz, E.; Garín, J.; Orduna, J.; Horton, P. N.; Hursthouse, M. B. *J. Am. Chem. Soc.* **2010**, *132*, 1706.

(48) Coe, B. J.; Harris, J. A.; Asselberghs, I.; Wostyn, K.; Clays, K.; Persoons, A.; Brunschwig, B. S.; Coles, S. J.; Gelbrich, T.; Light, M. E.; Hursthouse, M. B.; Nakatani, K. *Adv. Funct. Mater.* **2003**, *13*, 347.

(49) See for example: Orr, B. J.; Ward, J. F. *Mol. Phys.* **1971**, *20*, 513.

(50) See for examples: (a) Powell, C. E.; Morrall, J. P.; Ward, S. A.; Cifuentes, M. P.; Notaras, E. G. A.; Samoc, M.; Humphrey, M. G. *J. Am. Chem. Soc.* **2004**, *126*, 12234. (b) Samoc, M.; Samoc, A.; Humphrey, M. G.; Cifuentes, M. P.; Luther-Davies, B.; Fleitz, P. A. *Mol. Cryst. Liq. Cryst.* **2008**, *485*, 994.

(51) See for examples: (a) Das, S.; Nag, A.; Goswami, D.; Bharadwaj, P. K. *J. Am. Chem. Soc.* **2006**, *128*, 402. (b) Drobizhev, M.; Stepanenko, Y.; Rebane, A.; Wilson, C. J.; Screen, T. E. O.; Anderson, H. L. *J. Am. Chem. Soc.* **2006**, *128*, 12432. (c) Kim, K. S.; Noh, S. B.; Katsuda, T.; Ito, S.; Osuka, A.; Kim, D.-H. *Chem. Commun.* **2007**, 2479. (d) Collini, E.; Mazzucato, S.; Zerbetto, M.; Ferrante, C.; Bozio, R.; Pizzotti, M.; Tessore, F.; Ugo, R. *Chem. Phys. Lett.* **2008**, *454*, 70. (e) Jana, A.; Jang, S. Y.; Shin, J.-Y.; Kumar De, A.; Goswami, D.; Kim, D.; Bharadwaj, P. K. *Chem.—Eur. J.* **2008**, *14*, 10628. (f) Roberts, R. L.; Schwich, T.; Corkery, T. C.; Cifuentes, M. P.; Green, K. A.; Farmer, J. D.; Low, P. J.; Marder, T. B.; Samoc, M.; Humphrey, M. G. *Adv. Mater.* **2009**, *21*, 2318. (g) Odom, S. A.; Webster, S.; Padilha, L. A.; Peceli, D.; Hu, H.-H.; Nootz, G.; Chung, S.-J.; Ohira, S.; Matichak, J. D.; Przhonska, O. V.; Kachkovski, A. D.; Barlow, S.; Brédas, J.-L.; Anderson, H. L.; Hagan, D. J.; Van Stryland, E. W.; Marder, S. R. *J. Am. Chem. Soc.* **2009**, *131*, 7510. (h) Webster, S.; Odom, S. A.; Padilha, L. A.; Przhonska, O. V.; Peceli, D.; Hu, H.-H.; Nootz, G.; Kachkovski, A. D.; Matichak, J.; Barlow, S.; Anderson, H. L.; Marder, S. R.; Hagan, D. J.; Van Stryland, E. W. *J. Phys. Chem. B* **2009**, *113*, 14854. (i) Padilha, L. A.; Webster, S.; Przhonska, O. V.; Hu, H.-H.; Peceli, D.; Ensley, T. R.; Bondar, M. V.; Gerasov, A. O.; Kovtun, Y. P.; Shandura, M. P.; Kachkovski, A. D.; Hagan, D. J.; Van Stryland, E. W. *J. Phys. Chem. A* **2010**, *114*, 6493.

(52) Xu, X.-L.; Qiu, W.-W.; Zhou, Q.; Tang, J.; Yang, F.; Sun, Z.-R.; Audebert, P. *J. Phys. Chem. B* **2008**, *112*, 4913.

JP106473E